Experimental study of heat transfer at the transition regime between the natural convection and nucleate boiling: Influence of the heated wall tilt angle on the onset of nucleate boiling (ONB) and natural convection (ONC)

Lounès Tadrist, Hervé Combeau, Mohammed Zamoum, Mohand Kessal

Experimental study of Heat transfer at the transition regime between the natural convection and nucleate boiling: Influence of the heated wall tilt angle on the Onset of nucleate boiling (ONB) and Natural convection (ONC)

Lounès Tadrist[1*], Hervé Combeau[2], Mohammed Zamoum[1,3], Mohand Kessal[3]

[1]Aix-Marseille Université, CNRS, Laboratoire IUSTI, UMR 7343, Technopôle de Château Gombert, 13453 Marseille Cedex 13, France

[2]Institut Jean Lamour, Dép. SI2M, UMR CNRS 7198 – Université de Lorraine, Parc de Saurupt CS 50840, F-54011 Nancy cedex, France

[3]Laboratoire Génie Physique des Hydrocarbures LGPH, Faculté des Hydrocarbures et de la Chimie FHC, Université M'hamed Bougara UMBB, Boumerdès, 35000, Algérie

lounes.tadrist@univ-amu.fr, herve.combeau@univ-lorraine.fr, m_zamoum2000@yahoo.fr, m.kessal@voila.fr

Abstract

The works carried out in this study aimed to get a better understanding of the heat transfer in natural convection and nucleate boiling as well as the transition between these two regimes. An experimental test set up was built to generate the liquid boiling on the wall using a boiling-meter. This sensor was developed in order to investigate the heat transfer and its dependence with time in well controlled conditions. Temperature, pressure and heat flux required for the measurements were implemented. Experiments were focused on determining the characteristic curves of heat transfer in the natural convection regime and the nucleate boiling regime. The influence of the orientation of the wall relative to the gravity on the heat transfer is investigated. Characteristic heat transfer curves were obtained in several operating conditions and wall orientation with regard to gravity.

At the transition regime between natural convection and nucleate boiling regimes, it was highlighted a competition between these two regimes. It was found, that the transferred heat flux differs depending on the orientation of the wall and the degree of liquid superheat in the nucleate boiling regime. In the natural convection regime, the measured heat fluxes exhibited a slight variation with the tilt angle of the wall. While in the nucleate boiling regime, strong variations were observed on the onset of nucleate boiling as well as for the heat flux. At very low heat flux, the heat transfer increases with the tilt angle while it decreases for moderate heat flux. The onset of nucleate boiling (ONB) and the onset of dominant natural convection (ONC) were found to decrease as a function of the tilt angle of the wall with different variation laws. The wall superheats values for the ONB and ONC are getting closer when the tilt angle tends to 180°.

Keywords

Boiling-meter, heat transfer, natural convection, nucleate boiling, surface inclination. ONB Onset Nucleate Boiling (ONB), Onset of Natural Convection (ONC).

1. Introduction

1.1 Context

The devices and systems used in many applications evolve towards a miniaturization of their size. This tendency has generated significant growth of micro and nanotechnologies. In the area of control and heat transfer enhancement, special attention is paid to the boiling heat transfer as it allows, for example, the dissipation of a large heat flux at low temperature differences. Such features proved to be of great interest in many fields of application, such as cooling of electronic components, industry of matter transformation and energy conversion.

The physical phenomena involved during boiling are complex and understanding their mechanisms in various operating conditions are essential for the control of heat transfer in many applications (Celata et al.[1]).

When a liquid is brought into contact with a wall maintained at a temperature above its saturation temperature, the boiling phenomenon may be triggered. It is manifested by the vapor formation at the wall as bubbles or a vapor film. The associated heat transfer is measured using characteristic curves of heat transfer. These latter are plotted by facing the heat flux density at the wall as a function of the wall superheat ΔT_{sat}. The shape of this curve has been established for the first time by Nukiyama [2] by immersing metallic wire heated by the Joule effect in a pool of distilled water. Since then, numerous publications on boiling phenomena were reported in the open literature. The objective of the works carried out was focused on the analysis of the physical phenomena and the determination of empirical correlations of heat transfer between the wall and fluid. In most cases, the authors provided characteristic curves of the heat transfer for applications such as the design of evaporators, steam generators, heat pumps, etc. Among these studies, several authors proposed correlations for evaluating the heat flux density based on the thermo-physical properties of the fluid and the wall (Forster and Zuber [3], Rohsenow [4], Forster and Greif [5], Han and Griffith [6], Cooper [7], Stephan Abdelsalam [8], Gorenflo [9]), etc.

According to thermal conditions applied on the wall, different flow patterns and boiling regimes exist. At small heat flux, natural convection takes place in the liquid. By increasing the heat flux, at a critical value, vapor bubbles appear at the wall. This corresponds to the onset of nucleate boiling (ONB). By increasing the heat flux, the nucleate boiling regime develops with the formation of a bigger bubble at the wall and vapor columns develop. For a critical heat flux

(CHF), the vapor film regime appears. For the imposed wall temperature, the boiling transition regime appears between the critical heat flux (CHF) and the Leidenfrost points (Carey [10]).
For decades, these flow patterns have been well identified. The influence of parameters such as the wall surface state, fluid properties, geometry of the wall and its inclination, level of gravity, on these regimes and the position of the characteristic points (ONB, CHF, etc.) are still very poorly understood. The major works published on the influence of the wall inclination on the heat transfer in nucleate boiling regime are reviewed in the following section.

1.2.1 Review on the influence of wall orientation on heat transfer

The first studies on the influence of wall orientation to the gravity vector on pool boiling, go back to those of Storr [11] in 1958. Littles and Wallis [12] and Chen [13] studied the heat transfer with refrigerant liquid such as Freon 113 or Freon 11. These authors observed an increase in the heat transfer when the wall is inclined. Chen [13] showed a decrease in heat transfer when the orientation angles varied from 150° to 180°.
Nishikawa et al. [14] determined the characteristic boiling curve for water on a copper plate at atmospheric pressure for a wall orientation varying from 0° to 175°. These authors showed a remarkable influence of the wall orientation on the heat transfer for low overheating. The heat flux increased with increasing the tilt angle. For high wall superheat, the inclination has less influence on the boiling curve. In addition, they noted an unlabeled effect of wall roughness on heat transfer. Beduz [15] reported results on nucleate boiling with nitrogen and found similar results to those reported by Nishikawa et al. [14].
El-Genk et al. [16] studied the boiling of water in transient state conditions as a function of wall superheat for several wall inclinations in the range 90°-180°. These authors reported boiling characteristic curves for different wall inclinations. The curves showed the same trends. At low wall superheat, the heat flux increases; while at higher wall superheat, the heat flux reaches a maximum and decreases. These authors showed that an increase in heat flux with the increasing wall inclination for low wall superheat. A reverse trend was observed for higher wall superheat.
Further investigations were carried out using dielectric fluids such as FC-72 and HFE at atmospheric pressure. Chang and You [17] conducted nucleate boiling experiments FC-72 on three heated surfaces (smooth, copper and aluminum particles deposit) on 10 x10 mm^2 surface for saturated conditions. On the smooth surface, they observed an increase in the heat flux with the inclination angle from 0° to 90° in the nucleate boiling regime. When the orientation angle was further increased from 90° to 180°, nucleate boiling heat transfer noticeably decreased at higher heat fluxes. For micro-porous-enhanced surfaces, nucleate boiling superheats were

found to be independent of wall orientation. Rainey and You [18] studied the effects of the size and orientation of the surface element on the heat transfer in nucleate boiling of FC-72 at atmospheric pressure. These authors showed that the nucleate pool boiling was affected by the heater orientation and size. The heat transfer increased slightly from 0° to 45° and then decreased dramatically from 90° to 180°. At low heat flux (< 3W/cm^2), they found better heat transfer rates with higher inclination angle up to 135°.

El-Genk and Bostanci [19] studied the boiling heat transfer of FC-72 and HFE-7100 at saturated conditions for structured surfaces with a porous layer. At low heat flux, they showed a very slight increase in the boiling curve as a function of inclination. At higher heat fluxes, the influence of tilt was more pronounced with an inverse trend to that observed at low heat flux. The heat transfer deteriorated with increasing angle from 0° to 180°. Priarone [20] carried out experiments to study boiling heat transfer for two fluids FC-72 and HFE-7100 and the tilt angles of the wall varying from 0° to 175°. He confirmed the trends observed by Nishikawa et al., [14] at low heat flux. At higher heat flux, the boiling curves intersect. Beyond this intersection point, the boiling curves showed inverse trends. The heat transfer decreased when the inclination angle increased.

Ho et al [21] conducted the experiments to investigate the effects of carbon nanotube (CNT) coated surfaces and the influence of surface orientations on saturated pool boiling heat transfer of FC-72 at atmospheric pressure. They reported that the boiling incipience heat flux for all orientations is 2.4 W/cm^2 for the CNT surface and 3.1 W/cm^2 for bare silicon which suggests that the heat flux required for initiating nucleate boiling is independent of the surface inclination. In addition, the incipience superheats are significantly lower for CNT surface as compared to bare silicon. On the other hand, the heat transfer performance decreases with increasing surface orientation whereas bare silicon exhibited improvement in heat transfer between 0° and 90° and deterioration in heat transfer between 90° and 180°.

Jun et al [22] studied the heater orientation effects at inclination angles from 0° (horizontal upward) to 180° (horizontal downward) on pool boiling heat transfer of saturated water using a durable high-temperature thermally-conductive microporous coating (HTCMC) created by sintering copper. They reported that the nucleate boiling heat transfer is enhanced at low heat fluxes as the inclination angle increases whereas the nucleate boiling heat transfer was similar at larger heat fluxes.

Jung and Kim [23] studied the effects of surface orientation on wall heat flux and bubble parameters in nucleate boiling of saturated water at atmospheric pressure and incorporating into the wall boiling model. The measured wall heat flux significantly increases with surface

orientation angle. A remarkable increase in nucleation site density and average bubble departure diameter were observed. Inclination of a boiling surface from horizontal to vertical increases nucleation site density by likely thickening thermal boundary layer and causes isolated bubbles to slide and coalesce with each other, thus forming a large merged bubble. On the other hand, they reported that the basic wall boiling model predicted relatively the very nominal increase with the surface orientation angle because the sub-correlations for bubble parameters related to evaporation and quenching heat transfer do not account for the orientation effects and only the enhanced convective heat transfer contributes to the wall heat flux increase.

Dadjoo et al [24] investigated the pool boiling of SiO2/water nanofluid over a copper flat plate heater at various inclinations of the heater surface. For both nanofluid and DI water, the results showed that increasing the inclination angle of the heater surface from 0° to 90° decreases the boiling heat transfer coefficient. These authors noted that surface roughness varies with the orientation of the surface. They reported that deposition of nanoparticles and bubble movements have important effects on nanofluid boiling over inclined surface.

Mei et al [25] experimentally investigated the effects of surface orientation and heater material on the heat transfer coefficient of nucleate boiling. Copper (Cu), stainless steel (SS) as well as prototype material (SA508) of the reactor pressure vessel in the nuclear power plant were used to perform the boiling tests under atmospheric pressure. The orientation angle of all boiling surfaces was varied between 0° (upward) and 180° (downward). The experimental results showed that the heat transfer coefficient increases with the increase of orientation angle in the low heat flux region and the orientation effect gradually reduces with the increase of heat flux for the boiling on the downward inclined surface.

1.2.2 Short review Onset of nucleate boiling (ONB)

Several investigations were carried out on bubble nucleation in different operating conditions. In the following section, we recall some of these studies.

Ahmadi et al [1] investigated the bubble dynamics at the onset of nucleate boiling in water subcooled flow boiling by using a high-speed camera. They compared the values of wall superheat at ONB with those obtained with theoretical relations or correlations of several authors (Davis and Anderson [2], Bergles and Rohsenow [3], Sato and Matsumura [4] and Basu et al [5]). The results show that the wall superheat at the onset of nucleate boiling was higher in the experiments under the atmospheric pressure.

Hale et al (2010) studied bubble characteristics in pool boiling on wetting liquid on smooth and rough surfaces. These authors highlighted an active nucleation site density with increasing wall

superheat and surface roughness. They compared their experimental results on the heat transfer with correlations proposed in the literature. They concluded no single correlation provides entire satisfactory predictions due to differences in the surface roughness exponent.

Nucleation during flow boiling in microchannels was investigated by Kandlikar (2006). This author compared his results to the existing theories. He found that the nucleation data points fall above the line representing the theoretical criterion derived by several authors.

More recently Masri et al [6] have studied experimentally the pool boiling heat transfer characteristics in saturation acetone conditions on rough and ultra-smooth surfaces of several aluminum samples. Depending on the characteristics of the surfaces, different types of boiling incipience are observed. They found in the case of an ultra-smooth surface, that huge superheats (80 K to 90 K) are required to start nucleate boiling.

In summary of this review, it should be noted that for plain surfaces and whatever the liquids were used for, most authors drew the same conclusion.

-For the nucleate boiling regime (isolated bubble regime), heat flux increases with the tilt angle of the hot wall relative to the 0° inclination angle (horizontal plate with an upward facing plate). There is a large increase in the heat flux according to the tilt angle for the water. The same tendency is found for dielectric fluid FC-72 and HFE-7100. For the fully developed nucleate boiling regime (bubble column regime) obtained at high heat flux, the results differ from one author to another. In case of water, the influence of the orientation of the heating wall on the heat transfer differs from one author to another. It has a minimal influence for some authors while for the others, an increase in the heat transfer is observed by increasing the tilt angle. Moreover, a group of authors reported a reverse sensitivity.

-For the onset of nucleate boiling area, very limited investigations were carried out. In their studies, authors didn't take into account for the ONB. this transition zone is probably difficult to investigate. This may be explained by the difficulty of accessing the accurate measurements with experimental devices implemented by several authors.

-All authors used a chamber containing the fluid and the heating element at the surface where boiling takes place. The measurement of the heat flux on the wall is deduced using the Fourier law from the measurement of a temperature gradient in the heating element assuming a well-known thermal conductivity. The influence of the orientation on boiling heat transfer is studied by pivoting the whole enclosure around a rotating axis. This operation is cumbersome and leads to different geometrical configurations of the fluid. Especially, the natural convection generated in the enclosure can be radically different from one orientation to another. Furthermore, this

technique of rotation influences the accuracy of the tilt of the measuring cell angle, in particular in the areas where boiling is extremely sensitive to the angle of inclination.

-The last point that might be mentioned is related to the operating conditions. The devices developed by several authors have a big size and a significant thermal inertia. As a result, a very long time is required to obtain thermal steady state conditions and limited operating conditions might be carried out.

1.3. Aim of the present study

The present work aims to better understand the heat transfer phenomena in natural convection and boiling regimes as well as the transition between these two regimes. To overcome the limitations discussed above in the accuracy and reproducibility of the results, we have designed a new experimental device allowing to study the influence of the main parameters on the boiling process such as the orientation of the heated wall, saturated conditions on heat transfer in nucleate boiling with well controlled operating conditions.

As the natural convection is a phenomenon that is present in all the situations encountered even in the boiling conditions, we precise for the reader that in this paper, we name natural convection regime, the situation in which no boiling occurs. For boiling regimes, we are aware that natural convection is still a phenomenon which participates in the heat transfer. Nevertheless, in this case, this regime is named nucleate boiling regime.

A lightweight boiling-meter that is easy to handle has been designed. This sensor measures the temperature and heat flux of the wall on which boiling takes place as a function of time. The experimental set up of this study has been designed specifically for this new sensor. The boiling-meter is mounted on a shaft rotatable around its axis from 0° to 360° with an accuracy of ± 0.5°. The influence of the orientation of the heated wall is thus managed without rotating the whole device. This new device opens up new perspectives which were not accessible to date with the existing devices. In particular, the unsteady effects of boiling heat transfer might be investigated with this new experimental set up. In a previous paper, preliminary results on nucleate boiling were presented (Zamoum et al. [34]). They demonstrated the feasibility of the measurements with the boiling-meter. This device was tested for single and multiple nucleation sites under well-controlled operating conditions.

In this paper, we present the results obtained using the proposed experimental device. We first describe the main components of the test cell and the boiling-meter. Then, the experimental results are presented. The characteristic curve of heat transfer in the natural convection and nucleate boiling regimes of FC-72 for different orientations of the wall are concerned. We also

present the hysteresis effect which is highlighted by conducting experiments with imposed ascending and descending heat flux. These results will be discussed and followed by a conclusion with the prospects emerging from this study.

2. Material and methods

The experimental device is designed to study the influence of various parameters on the boiling heat transfer with well-controlled operating conditions (thermodynamic, thermal and gravitational). In particular, the thermodynamic conditions of the fluid must be maintained under saturation conditions. The objective is therefore to produce the boiling process on a wall whose surface state is well-known and under well-controlled thermal conditions. To achieve these objectives, the device is constituted of several components. This is essentially the cell, surrounded by several elements to ensure the temperature control of the fluid, and the boiling-meter for measuring the temperature and heat flux level of the wall as a function of time where the boiling process occurs. Fig.1 shows a block diagram of the experimental device.

2. 1. The test cell and its environment

The test cell consists of a cubical enclosure having 100 mm side as schematized in Fig.2. The structure is made with Acetal Resin and the sides with transparent plexiglass. The dimensions of the square faces are 100mm side and 10mm thick. The Acetal and plexiglass were chosen for their heat transfer properties to minimize heat losses while permitting to view through all the phases of the boiling process. The internal volume of the cell is filled with 750 cm^3 of fluid (Perfluorohexane - Fluorinert FC-72). This cell is designed to be waterproof in the range of absolute pressures from 0.1 bar to 2 bars. Fig.2bis shows a side view of the boiling cell with several connections for the temperature control of the vapor and liquid phases while the boiling-meter placed in the center of the cell. We can see the liquid vapor interface in the upper part of the cell just below the blue line.

The cell in the liquid phase, is equipped with a heating resistor and a coil in which a secondary refrigerant circulates This coil is designed with a cooper tube with 2 mm diameter and placed as shown on fig 2 . The cooling fluid is water which is brought to the desired temperature (T_w= T_{sat} -5°C) using a cryostat. These two elements make it possible to maintain the liquid at the desired saturation temperature of the fluid when the boiling process occurs. In the vapor area, the heat exchanger, identical to the one situated in the liquid phase, is placed at 1 cm from the top of the test cell allows the condensation of the vapor produced by boiling and maintains the

fluid at the desired saturation temperature. The inlet water temperature in the heat exchanger is lower to the saturation temperature by 5 to 10°C ($T_w = T_{sat}$ -5/10°C depending on the operating conditions). For discharging the incondensable gas contained in the liquid, a jacketed tube is installed on the upper face of the enclosure. The central conduit, connected to the enclosure at one end, is occupied by the vapor and non-condensable gases from the gas dissolved in the liquid phase. The opposite end is connected to the atmosphere by a valve for removing non-condensable gases. In the annular zone, the refrigerant allows the steam contained in the gas mixture to be condensed and thereby separating non-condensable gases. These non-condensable gases are then discharged into the external environment by the upper valve from the pipeline.

The chosen fluid for studying the boiling phenomena is Fluorinert FC-72 (3M ™). It is a thermally and chemically stable fluid, its boiling temperature is relatively low (T_{sat}=*56.6°C;* P_{sat}=*1bar*). The used thermophysical properties of this fluid were taken from Mudawar [35]. The properties of the used fluid in the temperatures range considered (30-56.6°C) are given below in table 1.

Physical properties	ρ_l (kg/m^3)	ρ_v (kg/m^3)	k_l (W/mK)	ν_l (m^2/s)	C_{pl} (J/kgK)	L (J/kg)	γ (N/m)	P_{sat} (Bar)
T=30°C	1669.1	5.27	0.052	$3.6\ 10^{-7}$	1057.3	91804	$1.1\ 10^{-2}$	0.366
T=40 °C	1649.6	7.63	0.054	$3.2\ 10^{-7}$	1072.8	89147	$9.7\ 10^{-3}$	0.546
T =56,6°C	1619.8	13.36	0.0521	$2.8\ 10^{-7}$	1098.4	84515	$8.3\ 10^{-3}$	1.002

Table 1 Liquid and saturated vapor properties of FC 72 [35]

Physical properties	ρ_v (kg/m^3)	k_v [38] (W/mK)	ν_v [36] (m^2/s)	C_v [37] (J/kgK)
T=37°C	6,88	$5\ 10^{-3}$ to $15\ 10^{-3}$	$1.63\ 10^{-6}$	778
T =56,6°C	13,4	$5\ 10^{-3}$ to $15\ 10^{-3}$	$8,73\ 10^{-7}$	-

Table 2 vapor properties of FC 72 [36] and [37] [38]

The properties of the saturated vapor are scarce. The values found in the open literature are presented in table 2. For the thermal conductivity, as no values are available in the literature, we adopted the limits values measured for several hydrocarbons (Fellows et al. [38]).

The operating conditions for the investigations are easier to achieve using this fluid justifying the choice of the studied fluid. To ensure a uniform temperature in the liquid phase, a magnetic stirrer placed at the bottom of the enclosure in the liquid zone that homogenizes the fluid

temperature before each experiment. The fluid temperature in the enclosure is measured with four K-type thermocouples. The pressures in the enclosure are measured using two SCX 15DN type sensors. One pressure sensor placed in the vapor zone allows measuring the vapor pressure and another is placed in the lower part of the cell allows the pressure measurement in the liquid zone. The boiling-meter located inside the enclosure in the liquid zone allows the boiling process to occur on the upper surface of the flux-meter (Fig.3) as well as to analyze the different mechanisms of bubble nucleation, bubble dynamics and heat transfer. The boiling-meter was designed to allow tilting the wall where the boiling takes place with an angle ranging from 0° to 360°.

2.2. The boiling-meter

This device is designed and manufactured in a cylindrical-shape. It consists of three ultrathin flux-meters, two copper wafers and a resistive layer to cause heating of the wall by Joule effect (Fig.3). The flux-meters are designed by the Captec company (http://www.captec.fr). Two identical flux-meters are placed on the top and the underside. Each flux-meter is shaped as a circular disk of 20 mm in diameter and 0.4 mm thick, instrumented with a heat flux-meter and temperature sensors. The first measures the heat flux transmitted to the fluid while the second measures the surface temperature. The third flux-meter rectangular shape of 50 mm length, 5 mm width and 0.4 mm thick is installed on the side edge of the boiling-meter. This sensor measures the heat flux transmitted through the side surface of the boiling-meter. This device allows investigations of heat transfer in natural convection as well as in boiling conditions regimes.

The boiling wall is the upper side of heat flux-meter made by a copper material (Fig.3). This choice is made in order to measure the heat transfer characteristics (heat flux and temperature) on the wall where the boiling process takes place. The surface of the boiling wall is made as smooth as possible. To this end, it is polished using an Emery cloth (grains 240 and 1200) and finally with a lens tissue with liquid diamond.

Fig.4a shows a sample of the boiling wall surface obtained an optical microscope. On this picture, the reference length is 20μm. At this scale, one can see the surface state which presents a non-uniform roughness. The surface roughness was measured using a rough-meter type SJ 301-178-953D. Fig 4b shows an example of the result obtained. Several measurements were carried out. The roughness value was found equal to Rp=0.47 ± 0.21 μm.

Boiling-meter design:

The boiling-meter is designed with a superposition of different components (three flux-meters, two copper wafers and a resistive film). The manufacturing of this element consisted of three phases. An assembly phase of all the components constituting this element using a conductive resin in a Teflon template. The assembly is placed in an oven at a temperature of 120 °C for four hours to fully solidify the resin. Once finished, the element is removed from the template. To stiffen the assembly and minimize lateral heat loss, the element is placed in a second Teflon plate, larger than the first one. It is then filled with an insulating resin of low thermal conductivity to have the same level with the upper surface of the boiling-meter. This assembly is again introduced into the furnace at 120 °C for four hours to solidify the resin. Once cooled, the element is removed from the template. The manufacturing of the device is finalized by the polishing operation of the planar surfaces using coarse sandpaper then finer grains. A final polishing operation is carried out using diamond in order to obtain smooth surfaces.

Boiling-meter time response

To analyze the response time of the boiling-meter placed in a liquid phase, we set an initial power (0.81W for the presented case) and started to record the heat flux and surface temperature delivered by the flux-meter device. After a while, the device reached steady state conditions (wall temperature and heat flux constant) as shown in Fig.5. At a chosen time, in these conditions, the electric power dissipated by the heater of the device is set to 1.12 W. We can see that the measured heat flux and wall temperature increase and tend to another steady state regime (Fig.5). This figure shows the time evolution of heat flux and temperature of the wall between the two imposed power values 0.81 W and 1.12 W in the horizontal position (results correspond to the wall facing upward). Note that the response time is the same for heat flux and temperature. It is about 200 seconds where we observe that the first 100 sec after the increase in the power change is important, so that the increase in heat flux and temperature is less important for the last 100 seconds.

2.3 Instrumentation

The set of sensors located in the experimental device is connected to a datalogger type HP 34970A-permitting tracking all these quantities in real time with an optimum of 2 Hz acquisition frequency. The sensitivities of flux-meters are 2.82 $\mu V.W^{-1}.m^{-2}$ for the circular ones and 1.42 $\mu V.W^{-1}.m^{-2}$ for the rectangular. Programming these sensitivities in the datalogger enables direct reading of the heat flux density signal ($W.m^{-2}$). With the acquisition Agilent BenchLink, the data are recorded in a text file, and then converted to an Excel file for

processing. The heat flux density is delivered with an accuracy of +/- 0.15 $KW.m^{-2}$ while those of the wall and the liquid temperature are delivered with an accuracy of +/- 0.2 °C.

The pressure sensors used are type SCX 15DN. This type of sensor has ± 1% pressure accuracy over a wide temperature range. It is calibrated and temperature compensated to provide a stable output signal in a temperature range of 0 °C to + 85 °C. It measures absolute, differential and relative pressures. These transducers were calibrated using a calibration device Druck DPI 605. The absolute pressure measuring range of the sensors is of 0.1 bar to 2 bars.
A visualization system of the nucleation surface is placed in front of the cell in order to view the entire surface. On one hand, this system consists of a high-speed camera coupled to a macro zoom lens in the horizontal axis of the cell, and on the other hand, an illumination system which varies according to the desired objective. The camera is simultaneously connected to a monitor to perform a control, and to a data acquisition card to record sequences on a computer.

2.4 Experimental Protocol

The experimental set-up is prepared before starting the experiments. The cell is partially filled with the test liquid Fluorinert (FC-72). At first, the non-condensable gases are removed from the liquid. The procedure used is to gradually heat the liquid using the immersed heating element while agitating the liquid using a magnetic stirrer. After a few moments, the temperature and pressure increase in the cell. As soon as the liquid is close to saturation conditions, vapor and non-condensable gases form. The vapor FC-72 and air mixture can be found in the upper region of the enclosure equipped with an exchanger in which the refrigerant circulates. A significant portion of the vapor is then condensed, and the other fraction mixed with the condensable gas is discharged from the enclosure through the dual condenser tube fitted with a manually operated valve. This operation is repeated several times to obtain the corresponding thermodynamic conditions of saturation of the pure fluid. The cartridge heater installed in the liquid zone of the chamber is then stopped. The fluid is naturally cooled to room temperature by the heat losses to the ambient temperature. As the chamber is sealed and the fluid is in saturation state, the decrease in temperature leads to the decrease in pressure. We check that the fluid is in saturation conditions for individual conditions by comparing the obtained saturation curve to the one delivered by the manufacturer 3M ™ (Fig.6). We then proceed to the boiling experiments.

For all the experiments carried out, the conditions consist in working with an imposed heat flux at the wall. Therefore, the wall temperature is a function of the heat transfer induced between the wall and the fluid. The heat power is delivered by a variable electrical power generator. The voltage varies in the range 0-15V with a maximum intensity of 2A. The maximum heat power dissipated by Joule effect is 30 W.

For each experiment, the heat is gradually brought with the resistive film located in the heart of the boiling-meter. Low heat flux values are needed since the boiling is generated in a liquid under saturation conditions.

Each experiment consists of imposing a constant power dissipated by the Joule effect in the heating element. This heat is transferred to the fluid across the surface of the boiling-meter. The set of thermal and thermodynamic data, the measured heat flux and temperature of the nucleation surface of the boiling-meter, the temperature and pressure of the fluid, are recorded. The dynamics of boiling created on the wall of the boiling-meter have also been filmed using a camera (see fig.17 and 18). This operation is repeated for several thermal input values over the available range. The limitations are mainly due to the resistance of the materials constituting the enclosure and the boiling-meter. In the present study, the limiting temperature to preserve the heating element of the boiling-meter should not exceed 100 °C.

Boiling heat transfer curve procedure for a saturation temperature 36 °C:

As the operating temperature of the liquid FC-72 pool was expected to be at 36 °C which is above the ambient temperature, we heated the FC-72 to the operating saturation temperature by using the heating element which is connected to a regulation system (set at 36 °C). Initially the heat exchangers are not enabled. After reaching a homogeneous temperature distribution in the liquid and vapor phases, the experimental heat transfer characteristic points are carried out and the associated curves are deduced. To determine these curves, heat generated by the Joule effect is gradually brought with the resistive film located in the heart of boiling-meter. Heat transfer takes place between the boiling-meter and the FC-72 in liquid state. Once the steady state is reached, the set of thermal and thermodynamic data: the heat flux at the nucleation wall, the temperature of the nucleation wall, the temperature and pressure of the liquid pool are recorded. This operation is repeated for several thermal input values over the available range. At relatively high heat generation, the fluid temperature exceeds 36 °C and the heating element is switched off automatically. Thus, the liquid saturation temperature will no longer be regulated by the heating element into the liquid, but by the two exchangers situated in the liquid and vapor phases

of the test cell. These two exchangers allow the control of the desired saturation temperature of the fluid.

Once the maximum value of the heat power generated by the Joule effect is reached, the heat transfer characteristic curve for a decreasing heat flux is determined. We gradually diminish the power dissipated in the heart of the boiling-meter, while maintaining the saturation temperature in the cell with the two heat exchangers as already mentioned above. For each imposed power, all the data are recorded when a steady state regime is established. For the interest of the study, this operation is repeated for several heat power generation values until the lowest heat power generation is reached.

Reproducibility of experiments:
As we stated in the introduction, the goal of this work is to study the influence of the orientation of the surface relative to the gravity on boiling heat transfer. Therefore, we worked with the same surface without being altered. To check this point, experiments were performed for several days under the same operating conditions. Fig.7 shows an example of the boiling curve of FC-72 at a saturation temperature of 36°C on a horizontal wall oriented upwardly over several days' intervals. One can notice that the boiling curves remain unchanged, thereby confirming that the nucleation surface and the operating conditions remain unchanged to give reproducible results.

3. Results and discussion

The experimental setup allows investigating the heat transfer phenomena in a natural convection regime and in a nucleate boiling regime on a surface (multisite for nucleation). As a validation of the device, the heat transfer characteristic curves at imposed increasing and decreasing heat flux and for an inclination angle of 0° are presented and discussed. Notably, the effect of hysteresis is highlighted. Then, we analyzed the regime of heat transfer with the help of the measured heat flux exchanged between the heated wall and the liquid, the heating wall temperature and the liquid temperature. Then, the averaged behaviors of the heat transfer are determined. For a better understanding of the involved phenomena, experiments at various inclinations of the heated wall were conducted.

3.1 Heat transfer characteristic curves: hysteresis effect

In this paper, only one saturated condition of the fluid is presented in order to investigate in detail the influence of the tilt angle of the plate on the heat transfer characteristic curve. The saturated conditions investigated are T_{sat}=36°C, p_{sat}=0.48 bar. Moreover, for this point, the operating conditions are easily controlled, and the experiments are easier to carry out. This point constitutes a good compromise between the heat loss reduction and the boiling-meter safety. The ideal point corresponds to a saturation temperature close to the ambient temperature (25°C, 0.3 bar). In this case the saturation pressure is low and may provoke safety problems and leakage.

In Fig.8, the heat transfer characteristic curves of the FC-72 for an imposed increasing and decreasing heat flux from the top side on a horizontal wall in contact with the liquid in saturation conditions T_{sat}=36°C, p_{sat}=0.48 bar are presented. These curves represent the variation of the heat flux measured for different values of heating power imposed on the basis of the temperature difference ΔT_{sat} between the temperature of the wall T_w and the liquid saturation temperature T_{sat}.

In the case of an increasing heat flux, different regimes can be observed depending on ΔT_{sat} ranges: in the range of 2.5 to 17.5 °C, the heat flux is low and varies continuously as a function of the temperature difference ΔT_{sat}. In this ΔT_{sat} range, the observations of the fluid flow revealed the presence of plumes. The heat transfer takes place mainly by natural convection. For ΔT_{sat} values in the range of 19 °C to 38.5 °C, the heat transfer is governed by nucleate boiling. In this range, the heat flux increases linearly with ΔT_{sat} and the heat transfer is more efficient compared to that of the natural convection regime. Between these two distinct zones, there is a transition zone. In this zone, the heat flux varies in a non-monotonic way with the temperature difference ΔT_{sat}. One can observe an increase in the heat flux when ΔT_{sat} decreases. As a result, vapor bubbles start to be visible. The number of bubbles increases when the heat flux increases.

For decreasing the heat flux of the heat transfer characteristic curve, starting from the maximum value of the heat flux in the nucleate boiling regime, the characteristic curve of the heat transfer is continuous and superimposed on that obtained when the heat flux is increased. In the transition zone and the natural convection zone, the two heat transfer characteristic curves (for decreasing and increasing heat fluxes cases) tend to join when the temperature difference ΔT_{sat} becomes very small. Thus, a hysteresis effect appears. This is located in between the onset of nucleation boiling (ONB) (q_{crit}=6.5 kW.m^{-2}) to a flux density of 2.5 kW.m^{-2}. The point

corresponding to the highest value of the heat flux in the natural convection regime will be called: Onset Natural Convection (ONC).

3.2 Characterization of the heat transfers in natural convection and nucleate boiling regimes

We discuss in the following part the time evolution of the heat flux, the temperature of the wall and the fluid saturation temperature for three different conditions (A, B, C). These points, indicated on the boiling curve in Fig.8, are obtained for FC-72 on a wall with an inclination angle equal to 0° for an increasing exploration of the heat flux.

Point A is located in the region of the natural convection regime, the point C in the nucleate boiling regime and point B in the transition zone.

The mean values, the standard deviation, the minimum and maximum values and the difference between these two last values (range) for the heat flux density at the wall, the wall temperature and the average pool temperature of the FC-72 recorded for the three points A, B, C are given respectively in table 2A, 2B, and 2C. Their time evolutions are plotted in Fig. 9a, b, c. For the three points A, B, C, fluctuations are observed for all the measured quantities. Fluctuation levels for the pool temperature of the FC-72 are low and in the order of temperature measurement error. The fluctuations of the wall temperature are within the range [0.5 °C, 1.35 °C] which corresponds to greater values than the error on temperature measurement. Thus, these fluctuations may be related to physical phenomena. For the point A, corresponding to the natural convection regime, the fluctuations of the wall temperature are the lowest (0.5 °C). The most important fluctuation values are observed for point C located in the nucleate boiling regime. For the point C, it is remarkable to notice the existence of two temperature steps shifted by 1°C. The holding times on each temperature step are of the same order of magnitude of 10 seconds. Therefore, it seems that there are two different heat transfer mechanisms at the wall probably due to the interaction between the formation and motion of bubbles on the heated surface and the natural convection at the enclosure scale. Fluctuations in the heat flux measured for the three points (A, B, C) are of the same order of magnitude, they vary in the interval [369, 548] $W.m^{-2}$. The width of this heat flux interval is of the same order of magnitude than the measurement error with ± 150 $W.m^{-2}$. These results show that with this experimental device, it is possible to perform a time dependent analysis of heat transfer in the different regimes. A thorough analysis of this type is however not in the scope of this paper. Indeed, such an analysis would require a theoretical study of the natural convection at the whole enclosure scale and its coupling with the boiling-meter.

Table 2A

POINT A	*Mean*	*sd(Er±)*	*Min*	*Max*	*Range*
Heat Flux(Wm-2)	*2823*	*85.4*	*2636*	*3005*	*369*
Tsat(°C)	*36.6*	*0.036*	*36.49*	*36.69*	*0.20*
Tw(°C)	*45.9*	*0.122*	*45.70*	*46.22*	*0.52*

Table 2B

POINT B	Mean	sd(Er±)	Min	Max	Range
Heat Flux (Wm^{-2})	6363	107	6173	6721	548
T_{sat}(°C)	36.57	0.027	36.51	36.63	0.12
T_w(°C)	54.04	0.143	53.66	54.37	0.71

Table 2C

POINT C	Mean	sd(Er±)	Min	Max	Range
Heat Flux(Wm-2)	28752	84	28523	28943	420
Tsat(°C)	36.58	0.024	36.54	36.66	0.12
Tw(°C)	68.15	0.436	67.48	68.83	1.35

3.3 Characterization of heat transfer averaged in time

The analysis of the time evolution of the temperatures and heat flux made in the previous section shows the existence of stable average values in time for all of these variables. It is thus possible to analyze the average characteristic values of heat transfer and access to a heat transfer coefficient representative of an average condition for all the regimes. First of all, we compared our experimental results with those given by the correlations from literature for natural convection and nucleate boiling regimes. Secondly, we propose an analysis of the transition zone between the natural convection and nucleate boiling regimes.

In natural convection, the correlation proposed by Fujii and Imura [39] for the estimation of the Nusselt number in the case of a horizontal plate heated in the upward direction has been used to determine the relation between the heat flux and the wall superheat. This correlation

expressed in terms of the heat flux versus the superheat is the following:

$$q = 0.16 k_L \left[\frac{g\beta}{\upsilon D_{TL}} \right]^{1/3} \Delta T^{4/3} \quad (1)$$

The comparison of the measured heat transfer characteristic curves with the correlation of equation (1) is presented in Fig.10 for the saturation condition: T_{sat} = 36 °C. The correlation for natural convection underestimates the heat flux for a given value of the wall superheat. It was already shown in Zamoum and Dubrac et al. [40] that a better estimation was obtained at lower saturation temperature. In fact, this correlation gives satisfactory results for the lower values of the saturation temperature while the heat transfer is underestimated for the higher saturation temperature. This phenomenon corresponds to the apparition of a macroscopic natural convection at the enclosure scale due to the temperature difference between the FC-72 and the environment. In the case of T_{sat} =36 °C, as the average ambient temperature is close to 20 °C, the temperature differences between T_{sat} and the ambient temperature start to be important and this is why the equation (1) underestimates the heat flux. This result is an indication that natural convection at the scale of boiling cell develops even in the case of no heat release from the boiling-meter. It results in an enhancement of the natural convection and of the heat transfer at the heated surface of the boiling-meter.

A large choice of correlation is possible to estimate the heat flux q as a function of the wall superheat ΔT_{sat} in the pool boiling regime. Among these, the commonly used are those proposed by Cooper [7], Stephan et al. [8] and Gorenflo [9]. The correlation of Stephan et al. is the least recent and the diversity of experimental measurements used makes it less precise. Gorenflo's investigation is regarded as the most reliable because it uses an experimental reference coefficient. The Cooper's correlation is more widely used due to its simplicity and to the fact that it uses only the reduced pressure and the molar mass to take into account for the physical properties of the fluids. Aprin et al. [41] conducted a detailed analysis about the consistency of the correlations proposed in the literature. They concluded that the correlations established by Cooper [7], Gorenflo [9] and Cornwell [42] fit well their experimental data. However, Cooper's correlation is the most appropriate as no adjustable parameter is necessary to predict their experimental results. As a result, the Cooper's correlation has been adopted for this study. The Cooper's correlation [7] can be expressed in the following form:

$$q = \left(55 p_r^{(0.12 - 0.2 log_{10} R_p)} (-log_{10}(p_r))^{-0.55} M^{-0.5} (T_W - T_{sat}) \right)^3 \quad (2)$$

The curves in Fig.11 represent the evolution of the heat flux q versus the wall superheat ΔT_{sat} for different values of the roughness of the heating surface for a saturation temperature of 36°C. One can see the huge effect of the roughness on the results obtained with the Cooper correlation. Adopting a roughness of 0.3 μm, the Cooper's correlation is capable of reproducing the experimental results at low wall superheat. However, the dependence of the heat flux to a power 3 of the superheat gives an overestimation for the high wall superheat.

As we can see the measured value of the surface state Rp=0.47 ± 0.21μm differs from the value of 0.3 μm. This later value corresponds to the best agreement between the correlation and the experimental results for covering all the saturation pressures in the range of superheat close to the onset of nucleation boiling (ONB).

For the ONB we also compared our experimental results to relations proposed by several authors (Hsu [43], Davis et al [27], Bergles et al. [28] Sato et al [29] and Basu et al. [30]). All these relations give ONB values much lower than those measured. The correlation of Basu et al. [30], which introduced an empirical function, gives values higher than those measured.

The differences might be explained by the complex phenomena occurring at the wall and the correlations do not take into account these phenomena to predict the heat transfer. The surface state cannot only be taken by a given value of the roughness. Therefore, we proposed a new relation of the ONB which takes into account the interaction between the natural convection and the nucleate boiling regimes.

Fig.12 shows the evolution of heat flux versus the wall superheat measured and calculated with the correlation of equation (1) for the natural convection regime and from the Cooper's correlation for the nucleation boiling regime for T_{sat}=36°C. The intersection between the curves corresponding to the natural convection and that of the nucleation boiling occurs at a wall superheat equal to 15.4 °C which is close to the experimental value equal to 16.5 °C. Thus, an interpretation of this result is that the nucleate boiling regime starts when the heat transfer efficiency is greater in the nucleate boiling (NB) regime than in the natural convection (NC) regime.

We assume that this condition is satisfied when the nucleate boiling heat flux is higher than the natural convective one. The ΔT_{ONB} can thus be determined by using the criteria:

$$q_{NC}(\Delta T_{sat}) = q_{NB}(\Delta T_{sat}) \tag{3}$$

where q_{NC} is computed from equation (1) and q_{NB} from equation (2). It is then possible to get an explicit relation for ΔT_{ONB} in the case of a horizontal plate heated in the upward direction, it becomes:

$$\Delta T_{ONB} = \frac{0.333\left[\frac{g\beta}{\nu D_{TL}}\right]^{1/5} k_L^{3/5}}{(55 p_r^{(0.12-0.2\log_{10}(R_p))}(-\log_{10}(p_r))^{-0.55} M^{-0.5})^{9/5}} \quad (4)$$

From the expression of relation (4) of ΔT_{ONB}, the heat flux at the ONB can be determined. It becomes:

$$q_{ONB} = 0.16 k_L \left[\frac{g\beta}{\nu D_{TL}}\right]^{1/3} \Delta T_{ONB}^{4/3} \quad (5)$$

These results on the ONB suggest that the onset of nucleate boiling regime is not only linked to a nucleation problem, but from an interaction between the natural convection and boiling regimes. Indeed, for low superheat conditions at the wall, natural convection is dominant. Any possibility of bubble growth is neutralized by the fluid motion in the boundary layer scaled by natural convection. To reinforce this idea, we studied the influence of the orientation of the wall on heat transfer and ONB. A variation in the orientation of the wall will have the effect of altering the heat transfer in the natural convection and boiling regimes. This is the topic of the next section.

3.4 Influence of the tilt angle of the wall

After the degassing procedure of the FC-72 content in the test cell (see the experimental protocol part), we set the tilt angle of the heating surface in the horizontal position (angle 0°, wall heated from above), we then proceeded to boiling experiments. This allowed us to plot the heat transfer characteristic curves for an imposed increasing and descending heat fluxes for the FC-72 at a saturation temperature of 36 °C and a tilt angle of 0° of the boiling wall The time required for this experiment is one day. The day after, we moved to another tilt angle of the heating surface (45°). After confirming that the thermodynamic conditions (temperature, pressure) of the fluid remained unchanged and corresponded to a liquid vapor equilibrium by checking with the saturation curve shown in Fig. 6, we followed the same experimental protocol already used for the tilt angle 0°. After seven days of this operation (one characteristic

curve/day) we ended the determination of the heat transfer characteristic curves at imposed increasing and decreasing heat flux for the FC-72 at a saturation temperature of 36 °C for the following tilt angles: 0°, 45°, 90°, 135°, 170°, 175°, 180°. The results are now presented, in the next section for the ascending heat flux exploration.

3.5 Heat transfer characteristic curve for increasing heat flux

The heat transfer characteristic curves for increasing heat flux and for the tilt angle inclinations of: 0°, 45°, 90°, 135°, 170°, 175° and 180° are presented in Fig.13. With the exception of a tilt angle of the wall very close to 180° (at the accuracy of the angle measurement). We observe for all of these orientations, the existence of corresponding three zones as already discussed in section 3.2: a first zone corresponding to a natural convection regime, followed by a second zone of transition regime and leading to a third zone corresponding to nucleate boiling regime. In the natural convection regime, the heat transfer characteristic curves are very similar. Gradually as the tilt angle increases from 0° to 180°, the superheat required for boiling initiation (ONB) decreases (Fig.16). This decrease of the superheat is more important when the tilt angle becomes higher. Two types of behavior can be distinguished: for tilt angles from 0° to 135°, the ONB decreases slightly depending on the tilt angle; for tilt angles greater than 135°, the ONB decreases very strongly. The lowest value (5 °C) of the ONB is obtained for a tilt angle very close to 180°. While for a tilt angle value of 0°, the superheat at the boiling wall reaches the value of 17.5 °C.

For intermediate heat flux values $15 < q < 25$ kW.m^{-2}, there is a remarkable influence of the tilt angle of the wall on the heat transfer. The heat flux for a given superheat increases when the tilt angle increases. This effect has already been observed by Priarone [20] and Nishikawa et al. [44]. The first explanations of this behavior were given by Nishikawa et al. [14] and confirmed later by El-Genk et al. [19] and Priarone [20]. It was assumed that for the values of heat flux in this range, the heat transfer mechanism is dominated by the sliding bubbles along the boiling wall which thereby increases the heat flux transferred.

At higher heat flux values, the slopes of the characteristic curves are similar except for the larger values of the tilt angle for which the slope is lower. This effect is more pronounced for a tilt angle equal to 180°. These results can be interpreted due to a combination of several effects. The heat transfer mechanisms are governed by the boundary layer adjacent to the wall. The heat transfer increases as the renewal of vapor by the detachment of the bubbles is important. As the tilt angle increases, the bubbles size increases and their detachment frequency decreases. At

high tilt angles, this effect is more pronounced, thus tending to reduce the heat transfer. This effect is highlighted in Fig.13 where the boiling curve at a higher tilt angle crosses the one at a lower tilt angle.

3.6 Influence of the tilt angle of the boiling surface on the heat transfer coefficient

From Fig.13, we can deduce the variation of the heat transfer coefficient ($h = q / \Delta T_{sat}$) as a function of the wall superheat for various values of the tilt angle of the boiling surface. The results are shown in Fig.14. In this figure, we distinguish two zones defined by a sharp transition corresponding to the ONB. When the superheat at the wall is lower than ΔT_{ONB} (superheat at the ONB), the heat transfer coefficient varies slightly with the tilt angle. When the superheat is greater than ΔT_{ONB}, the heat transfer coefficient evolves differently with the superheat depending on the orientation of the wall. For a tilt angle in between 0° and 135°, the heat transfer coefficient increases with the superheat. For tilt angles in between 135° and 175°, the heat transfer coefficient remains substantially constant. Finally, to the neighboring tilt angle of 180°, it decreases according to the superheat. Thus, the effect of an increase in the wall superheat on the intensification of heat transfer differs depending on the orientation of the wall. Notably for the high tilt angles, the heat transfer enhancement is higher just after the ONB.

3.7 Heat transfer characteristic curves for decreasing heat flux

Fig.16 shows the heat transfer characteristic curves as measured in the case of decreasing heat flux for various orientations of the boiling wall. These curves are obtained after reaching the maximum values of heat flux for increasing heat flux. Their monotonous behavior is common in all these curves when varying ΔT_{sat}. These curves differ to those obtained at increasing heat flux in which a sharp variation is observed at the ONB. In addition, for a given tilt angle, the descending heat transfer characteristic curves are located above the heat transfer characteristic curve for increasing heat flux at low superheat and are identical in the nucleate boiling regime.

3.8 Discussion

The above results confirm that nucleation is not the main phenomenon that controls the ONB but rather a competition between natural convection and boiling. For increasing heat flux and for low superheat, natural convection is the dominant regime for the heat transfer. The possibility of bubble growth is neutralized by the fluid motion in the natural convection boundary layer. Conversely, for decreasing heat flux, a natural convection regime cannot be set

up and by this way, the emission of bubbles cannot be stopped abruptly. It results a delay of the onset of the natural convection regime. Below a certain value of superheat, the heat transfer characteristic curves for the two exploration sides for the heat flux are identical. This suggests that the natural convection regime becomes dominant. The point of ONC is shown in Fig.16. It is observed in Fig.16 that the ONC wall superheat decreases almost linearly as a function of tilt angle. This variation is radically different from ΔT_{ONB} when increasing heat flux.

It has been possible to predict the superheat at the onset of nucleate boiling (ONB) by comparing the average heat transfer on one side by natural convection and on the other side in the nucleate boiling regime, for a tilt angle of the boiling-meter of 0° and for various values of saturation condition.

Regarding the effect of the tilt angle of the wall, the heat transfer in the natural convection regime is not strongly affected. This may be due to the fact that the natural convection at the scale of the whole enclosure is dominant. However, the boiling regime differs significantly according to the tilt angle. In particular, at 0°, the bubbles of millimeter size generated to trigger the boiling are produced at the wall at a high frequency. Under these conditions, the number of the nucleation site increases as a function of wall superheat. For a tilt angle in the vicinity of 180°, the bubbles generated at the wall grow laterally until a characteristic size of the order of the diameter of the boiling-meter. Under these conditions, the density of bubbles leaving the wall as well as their frequencies are significantly lower than for the 0° orientation (see Fig.17). The bubbles grow mainly laterally tending to drag the liquid laterally which forms a liquid film against the boiling surface. This superheated liquid film evaporates tending to increase the heat transfer at the wall. The natural convection intensity in the vicinity of the wall is lower for the orientation close to 180° than for 0°. For a tilt angle close to 180°, the bubbles appearing on the heated wall remain temporarily "confined" in this respect and will grow laterally until it reaches the dimensions of the size of the boiling-meter from which they are expelled by the gravity to the top of the enclosure. For a 0° orientation, the gravity effect distorts the bubbles longitudinally to the direction of gravity and the buoyancy forces are responsible for their detachment occurring at a bubble size of the order of one millimeter (see Fig.18). The difference between these two mechanisms can explain the lowest value of superheat at ONB for tilt angles close to 180°. This reasoning is reinforced by the stabilizing effect of gravity as the bubbles are confined within the wall for tilt angles close to 180° and which maintains the hot fluid at the wall.

Moreover, it must be noticed that for tilt angles close to 180°, the value of ΔT_{ONB} is close to that of ΔT_{ONC}. This can probably be explained by the fact that these transitions do not result from the competition between the heat transfer regimes (natural convection, boiling) but only by crossing an energy barrier that can be assumed to be related to the growth of a bubble in a cavity from a gas nucleus.

4. Conclusion

In this work, we have been able to characterize the heat transfer in a liquid under saturation conditions in the case of natural convection and nucleate boiling regimes. For this, we have implemented an experimental device with an original boiling-meter for measuring heat flux and temperature of the wall as function of time. This experimental set-up allows studying the heat transfer in natural convection and boiling regimes under well-controlled operating conditions and to provide reference heat transfer data.

The results presented in this article were obtained by exploiting the time average measured temperatures and heat flux. It has been possible to establish the heat transfer characteristic curves covering natural convection, nucleate boiling and transition regimes for different wall orientations.

For the natural convection regime, we have shown a significant influence of the saturation temperature on heat transfer. The orientation of the wall does not significantly alter the heat transfer coefficient. We attributed these results to the natural convection at the scale of the enclosure.

In the boiling regime, we highlighted the influence of the tilt angle of the surface on the heat transfer laws. At low superheat, the heat transfer is intensified with an increase in the inclination of the wall. At high superheat, this tendency is reversed.

Furthermore, we determined the superheat at ONB and ONC using a boiling-meter. We have shown that ΔT_{ONB} decreases with an increase in the saturation temperature. The same sensitivity was observed with an increase in the tilt angle of the wall. For a 0° tilt angle of the wall, we derived a law to predict ΔT_{ONB} based on a competition between the natural convection and nucleate boiling regimes. The predictions obtained from this law are in good agreement with the measured values.

These preliminary results lead us to continue understanding the ONB and ONC by developing an analysis of the heat transfer, on the one hand by the implementation of numerical simulations taking into account the natural convection at the enclosure scale and on the other hand by exploiting temporal signals of temperatures and heat flux associated with flow visualizations in the immediate vicinity of the wall.

Acknowledgements

Financial supports from ESA (European Space Agency) in the frame of the Microgravity Application Program and CNES (Centre National d'Etudes Spatiales) in the frame of GDR MFA (Groupement de Recherche Micropesanteur Fondamentale et Appliquée) are gratefully acknowledged.

Nomenclature

D_T	Thermal diffusivity	($m^2.s^{-1}$)
g	Gravity acceleration	($m.s^{-2}$)
k	Thermal conductivity	($W.m^{-1}K^{-1}$)
L	Latent Heat	(J/kg)
T	Temperature	(K)
M	Molar mass	($g.mole^{-1}$)
p_c	Critical pressure	(Pa)
p_r	Reduced pressure	
p	Pressure	(Pa)
q	Heat flux	($W.m^{-2}$)
Rp	Surface roughness	(µm)

Greek letters

β	Volumetric thermal expansion coefficient	(K^{-1})
ν	Kinematic viscosity	($m^2.s^{-1}$)
ρ	Density	($kg.m^{-3}$)
γ	Surface tension	($N.\ m^{-1}$)

Subscripts

B	Bubble
crit	Critical
L	Liquid
NB	Nucleate Boiling regime
NC	Natural Convection regime
ONB	Onset of Nucleate Boiling
ONC	Onset of Natural Convection
ref	Reference
sat	Saturation
W	Wall
V	Vapor

References

[1] G.P. Celata, C. Colin, P. Colinet, P. Di Marco, T. Gambaryan-Roisman, O. Kabov, O. Kyriopoulos, P. Stephan, L. Tadrist, C. Tropea, Bubbles, drops, films: transferring heat in space, Europhysics News, Vol 39, number 4, (2008), 23-25.

[2] S. Nukiyama, The Maximum and Minimum Values of the Heat Q Transmitted from Metal to Boiling Water under Atmospheric Pressure, J. Japan Soc. Mech. Eng., Vol. 37, no. 206, pp. 367-374, 1934. (english translation: Int. J. Heat Mass Transf., Vol. 9, pp. 1419-1433, 1966, and Vol. 27, 1984, 959-970.

[3] H.K. Forster, N. Zuber, Growth of a vapor bubble in a superheated liquid, Journal of Applied Physics, 25(4) (1954), 474–478.

[4] W.M. Rohsenow, A method of correlating heat transfer data for surface boiling of liquids, Transaction ASME, 84, (1962), 969–976.

[5] H. K. Forster, R. Greif, « Heat Transfer to a Boiling Liquid-Mechanism and Correlations », Journal of Heat Transfer, Vol. 81, pp. 43-54 ,1959

[6] C.Y. Han and P. Griffith; The mechanism of heat transfer in nucleate pool boiling–part I: Bubble initiation, growth and departure, International Journal of Heat and Mass Transfer. 8(6) (1965), 887–904.

[7] M.G. Cooper, Saturation nucleate pool boiling: a simple correlation, First U.K. National Conference on Heat Transfer, in: I. Chemical E. Symposium Series No. 86, (1984), 785-793.

[8] K. Stephan, M. Abdelsalam, Heat-transfer correlation for natural convection boiling, International Journal of Heat and Mass Transfer 23 (1980), 73–87.

[9] D. Gorenflo, Pool boiling, VDI Heat Atlas, (Chapter HA), pp. Ha1-Ha25, VDI-Verlag Gmbh, Dusseldorf Germany (1993).

[10] V.P. Carey, Liquid-Vapor Phase-change Phenomena, Second Edition, Ed. Taylor & Francis, (2008)

[11] A.T. Storr, The effect of heating surface geometry and orientation of nucleate boiling of subcooled water, M.S. Thesis, Washington University. Sever Institute of Technology, Department of Chemical Engineering. 1958.

[12] J.W. Littles, H.A. Wallis, Nucleate pool boiling of Freon 113 at reduced gravity levels, ASME paper, 70-HT-17 (1970).

[13] L.T. Chen, Heat transfer to pool-boiling Freon from inclined heating plate, Lett. Heat Mass Transfer 5 (1978), 111–120.

[14] K. Nishikawa, Y. Fujita, Satoru, and Ohta, Effect of surface configuration on nucleate boiling heat transfer, International Journal of Heat and Mass Transfer, 27(9) (1984), 1559–1571.

[15] C. Beduz, R.G. Scurlok, A.J. Sousa, Angular dependence of boiling heat transfer mechanisms in liquid nitrogen, Advance Cryogenic Engineering 33 (1988), 363-370.

[16] M.S. El-Genk, Z. Guo, Transient boiling from inclined and downward-facing surfaces in a saturated pool Rev. Int. Froid (1993) Vol 16 No 6 , 414-422.

[17] J.H. Chang, S.M. You, Heater orientation effects on pool boiling on micro-porous-enhanced surfaces in saturated FC-72. Journal Heat Transfer 118 (1996), 937–943.

[18] K.N. Rainey and S.M. You, Effects of heater size and orientation on pool boiling heat transfer from microporous coated surfaces. International Journal of Heat and Mass Transfer (44) (2001), 2589–2599.

[19] El-Genk, H. Bostanci, Saturation boiling of HFE-7100 from a copper surface simulating a microelectronic chip, International Journal Heat Mass Transfer 46 (2002), 1841–1854.

[20] A. Priarone, Effect of surface orientation on nucleate boiling and critical heat flux of dielectric fluids, International Journal of Thermal Science (44) (2005), 822–831.

[21] J.Y. Ho, K.C. Leong, C. Yang, Saturated pool boiling from carbon nanotube coated surfaces at different orientations, Int. J. Heat Mass Transf. 79 (2014), 893–904.

[22] S. Jun, J. Kim, S.M. You, H.Y. Kim, Effect of heater orientation on pool boiling heat transfer from sintered copper microporous coating in saturated water, Int. J. Heat Mass Transf. 103 (2016), 277–284.

[23] S. Jung, H. Kim, Effects of surface orientation on nucleate boiling heat transfer in a pool of water under atmospheric pressure, Nucl. Eng. Des. 305 (2016), 347–358.

[24] M. Dadjoo, N. Etesami, M.N Esfahany, Influence of orientation and roughness of heater surface on critical heat flux and pool boiling heat transfer coefficient of nanofluid, Applied Thermal Engineering, 124 (2017), 353–361.

[25] Y. Mei, Y. Shao, S. Gong, Y. Zhu, H. Gu, Effects of surface orientation and heater material on heat transfer coefficient and critical heat flux of nucleate boiling, Int. J. Heat and Mass Transf. 121 (2018), 632–640.

[26] R. Ahmadi, T. Ueno, T. Okawa, Bubble dynamics at boiling incipience in subcooled upward flow boiling International Journal of Heat and Mass Transfer 55 (2012) 488-497.

[27] E.J. Davis, G.H. Anderson, The incipience of nucleate boiling in forced convection flow, AIChEJ. 12 (1966) 774-780.

[28] A.E. Bergles, W.M. Rohsenow, The determination of forced-convection surface boiling heat transfer, J. Heat Transfer 1 (1964) 365-372.

[29] T. Sato, H. Matsumura, on the conditions of incipient subcooled boiling with forced convection, Bull. JSME 726 (1964) 392-398.

[30] N. Basu, G.R. Warrier, V.K. Dhir, Onset of nucleate boiling and active nucleation site density during subcooled flow boiling, J.Heat Transfer 124 (2002) 717- 728.

[31] J. P. McHale, and S. V. Garimella. "Bubble nucleation characteristics in pool boiling of a wetting liquid on smooth and rough surfaces." *International Journal of Multiphase Flow* 36.4 (2010): 249-260.

[32] S. G. Kandliar,. "Nucleation characteristics and stability considerations during flow boiling in microchannels." *Experimental Thermal and Fluid Science* 30.5 (2006): 441-447.

[33] M. Al Masri, S. Cioulachtjian, C. Veillas, I. Verrier, Y. Jourlin, J. Ibrahim, M. Martin, C. Pupier, F. Lefèvre, Nucleate boiling on ultra-smooth surfaces: explosive incipience and homogeneous density of nucleation sites, *Experimental Thermal and Fluid Science* (2017).

[34] M. Zamoum, L. Tadrist, H. Combeau, M. Kessal, Experimental study of boiling heat transfer on multiple and single nucleation sites using a boiling meter, Heat Transfer Engineering Vol 35(5), (2014), 508-516.

[35] Mudawar, T.M. Anderson, Parametric investigation into the effects of pressure, subcooIing, surface augmentation and choice of coolant on pool boiling in the design of cooling systems for high-power-density electronic chips, Journal of Electronic Packaging, (112), (1990), 375-382.

[36] McCoubrey, J. C., & Singh, N. M. Viscosity of some fluorocarbons in the vapor phase. Trans. Faraday Soc., 56, (1960) 486-489

[37] https://www.chemeo.com/cid/19-779-7/n-Perfluorohexane

[38] Fellows B.R., Richard R.G., Shankland I.R.- Thermal conductivity data for some environmentally acceptable fluorocarbons in Thermal Conductivity 21 , 1990 - book edited by Cremers C.J. and Fine H.A.

[39] T. Fujii, and H. Imura, Natural convection heat Transfer from a plate with arbitrary inclination, International Journal of Heat and Mass Transfer (15), (1972), 755-764.

[40] M. Zamoum, B. Dubrac, F.K. Goepper, L. Tadrist, H. Combeau, M. Kessal, Experimental study of transport phenomena at the onset of nucleate boiling using a boiligmeter, The 15th International Heat Transfer Conference (IHTC) Kyoto International Conference Center in Japan (2014).

[41] L. Aprin, P. Mercier, L. Tadrist, Local heat transfer analysis for boiling of hydrocarbons in complex geometries: A new approach for heat transfer prediction in staggered tube bundle, International Journal of Heat and Mass Transfer 54 (19) (2011), 4203-4219.

[42] K. Cornwell, D Houston, Nucleate pool boiling on horizontal tubes: a convection based correlation, International Journal of Heat Mass Transfer vol. 37, Suppl. 1, (1994), 303-309.

[43] Y. Y. Hsu, "On the size range of active nucleation cavities on a heating surface." *Journal of Heat Transfer* 84 (3) (1962), 207-213.

[44] K. Nishikawa, Y. Fujita, H. Ohta, S. Hidaka, Effects of system pressure and surface roughness on nucleate boiling heat transfer, Memoirs of the Faculty of Engineering, Kyushu University 42 (2) (1982), 95–111.

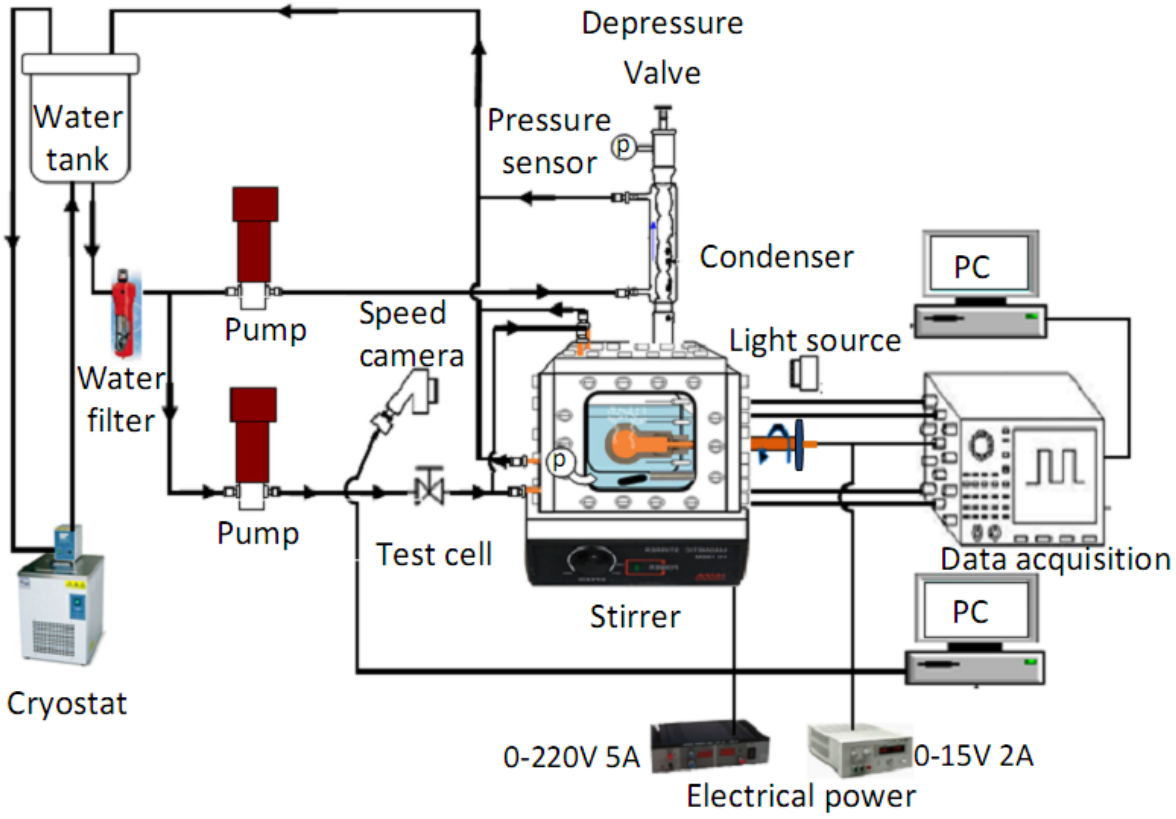

Figure 1: Overview of the experimental device constituted by the boiling cell, the instrumentation linked to the computer for the data acquisition and the temperature control of the cell.

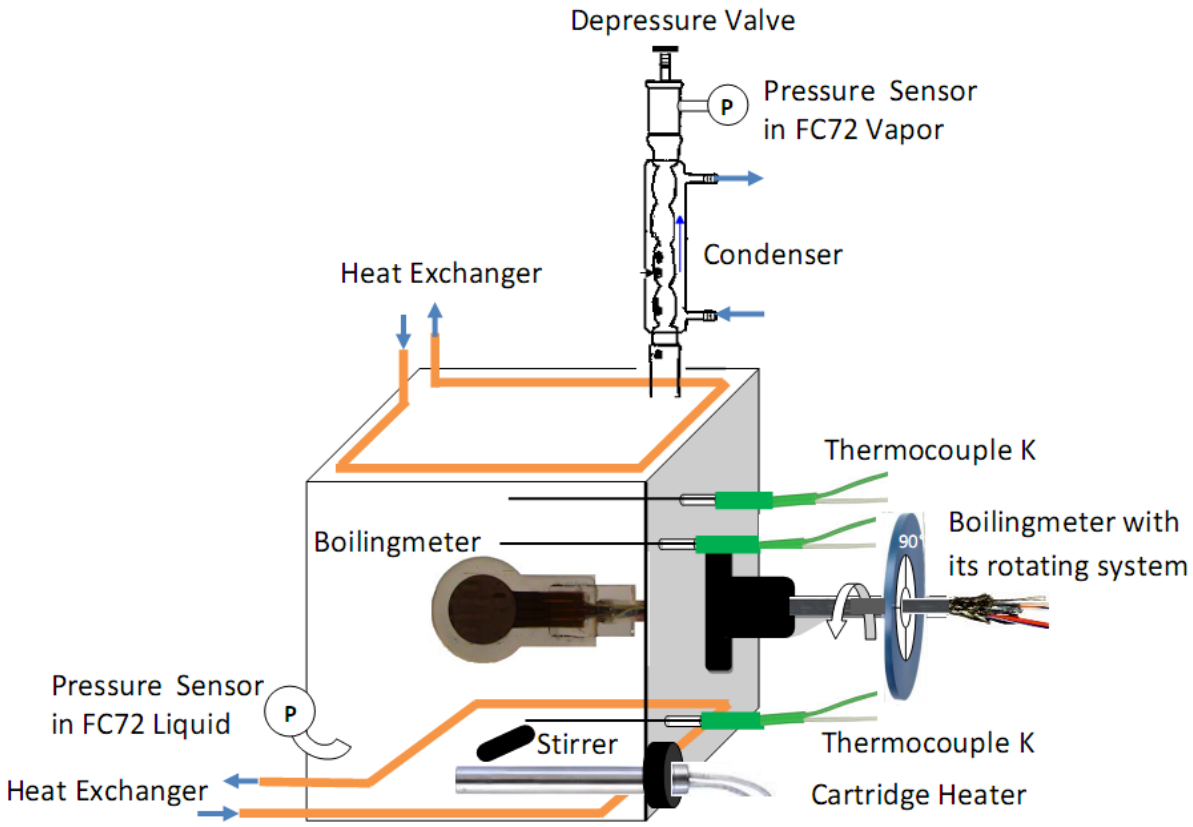

Figure 2: Boiling cell containing the boiling-meter as well as the instrumentation for temperature and pressure measurements. Two heat exchangers are installed for the control of the temperature in the liquid and vapor phases.

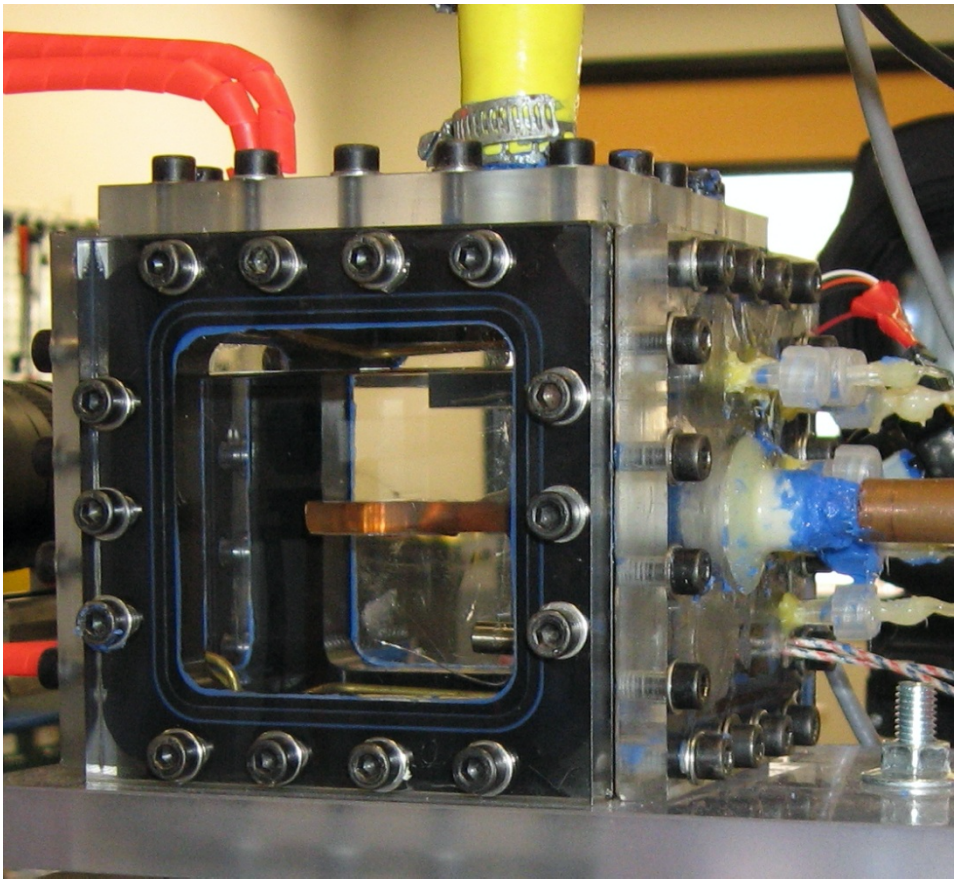

Figure 2 bis: Side view of the boiling cell with several connections for the temperature control of the vapor and liquid phases as well as the heat flux and temperature of the boiling-meter. The boiling-meter is placed in the center of the cell. The liquid vapor interface is visible in this view in the upper part of the cell.

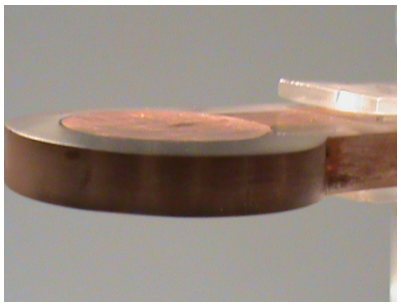

(a)

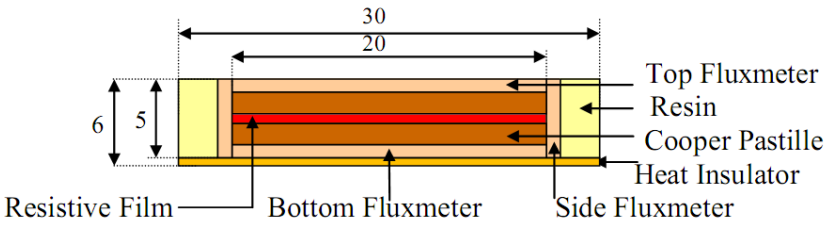

(b)

Figure 3: Photo and vertical section of the boiling-meter (a) Side view of the boiling-meter. The reflective part is the active surface for boiling. Sticking a thick Teflon piece on the opposite side deactivates the symmetrical surface area. The periphery of the boiling-meter is made with an insulating resin in order to prevent the boiling process on this area.
(b) Vertical section. The several components of the boiling-meter are detailed (given sizes are in mm)

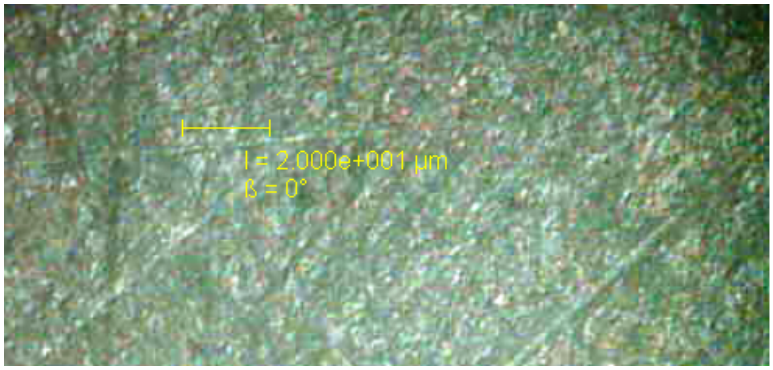

(a) Image of the surface (160μmx80μm)

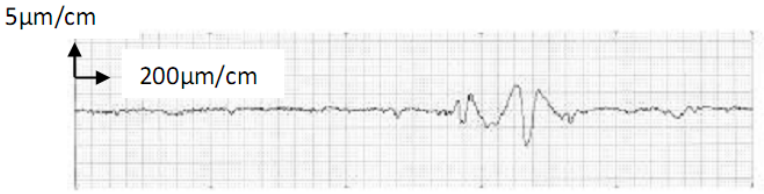

(b) Typical profile of the surface

Figure 4: Surface state of the boiling wall: (a) Image of the surface obtained with an optical microscope, (b) Typical surface roughness

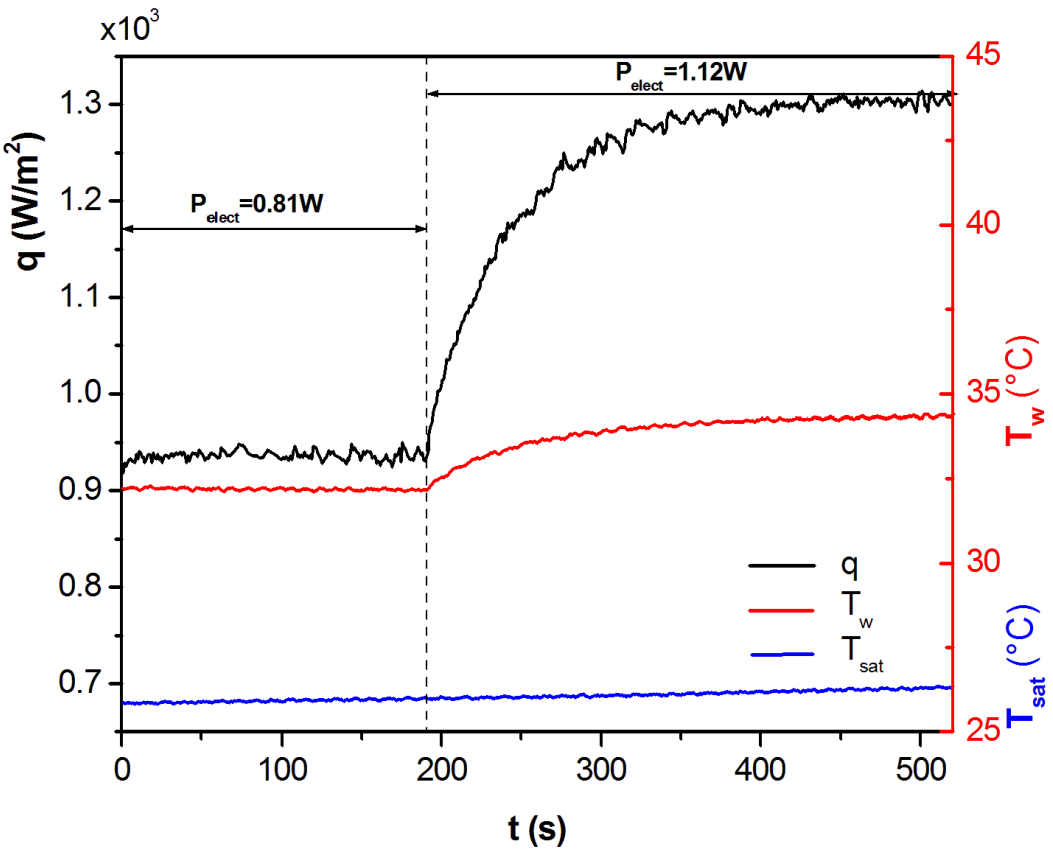

Figure 5: Time evolution of the temperature and the heat flux at the heated surface of the boiling-meter for a variation of the heat release by Joule effect from 0.81 W to 1.12 W. The blue curve represents the time evolution of the temperature in the liquid FC72 (T_{sat}=26°C)

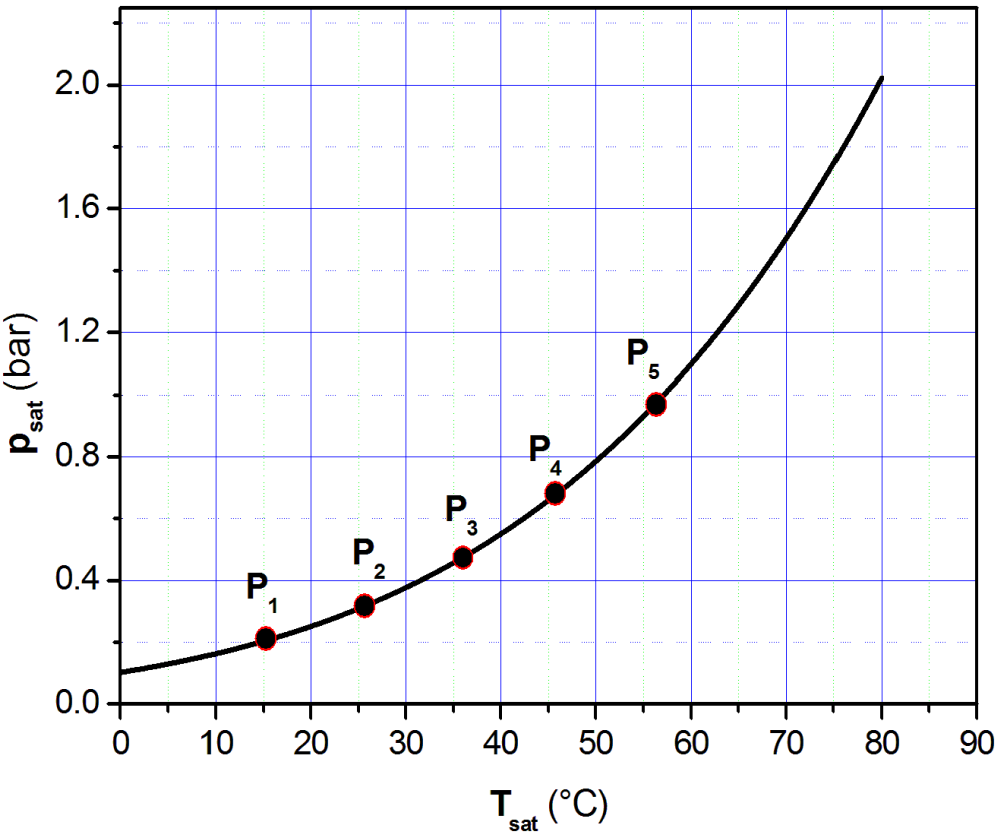

Figure 6: Saturation pressure P_{sat} versus saturation temperature for FC-72. The curve is given by 3M company. Dot points are those measured in the frame of the present study. A good agreement is found between present measurements and those given by 3M company.

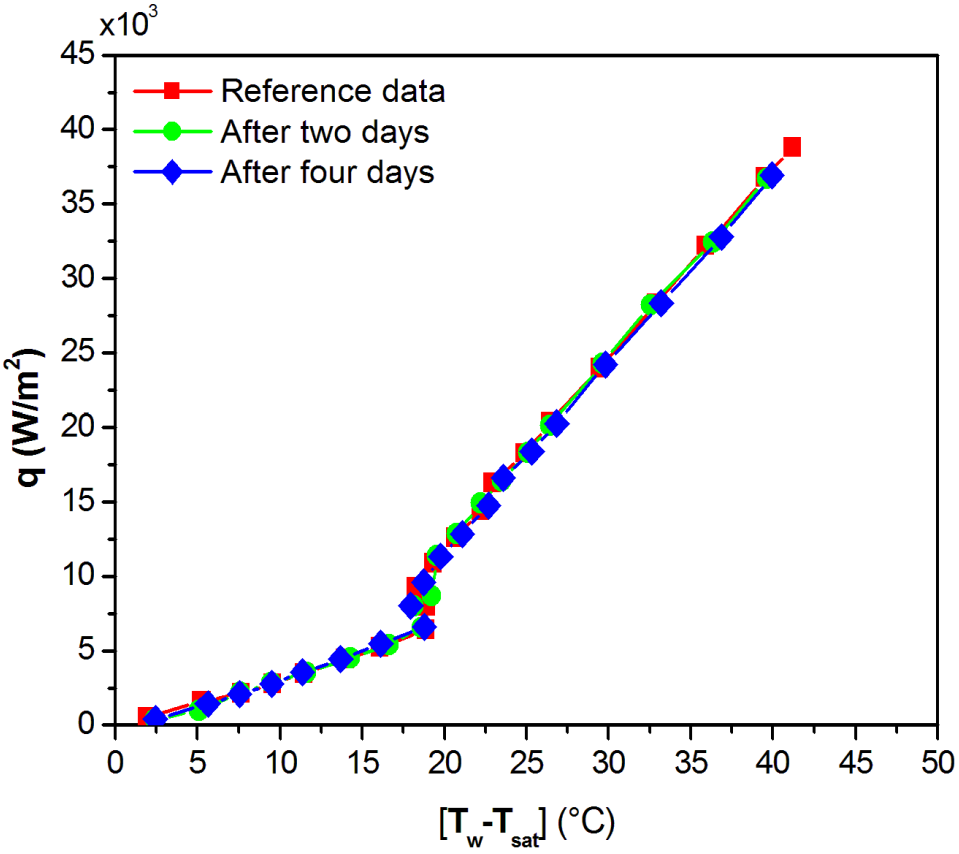

Figure 7: Heat transfer characteristic curves for an exploration with an ascending heat flux for the fluid FC72 and for a saturation condition (T_{sat}=36 °C, p_{sat}=0.48 bar). The three curves have been determined with an interval of two days between each experiment.

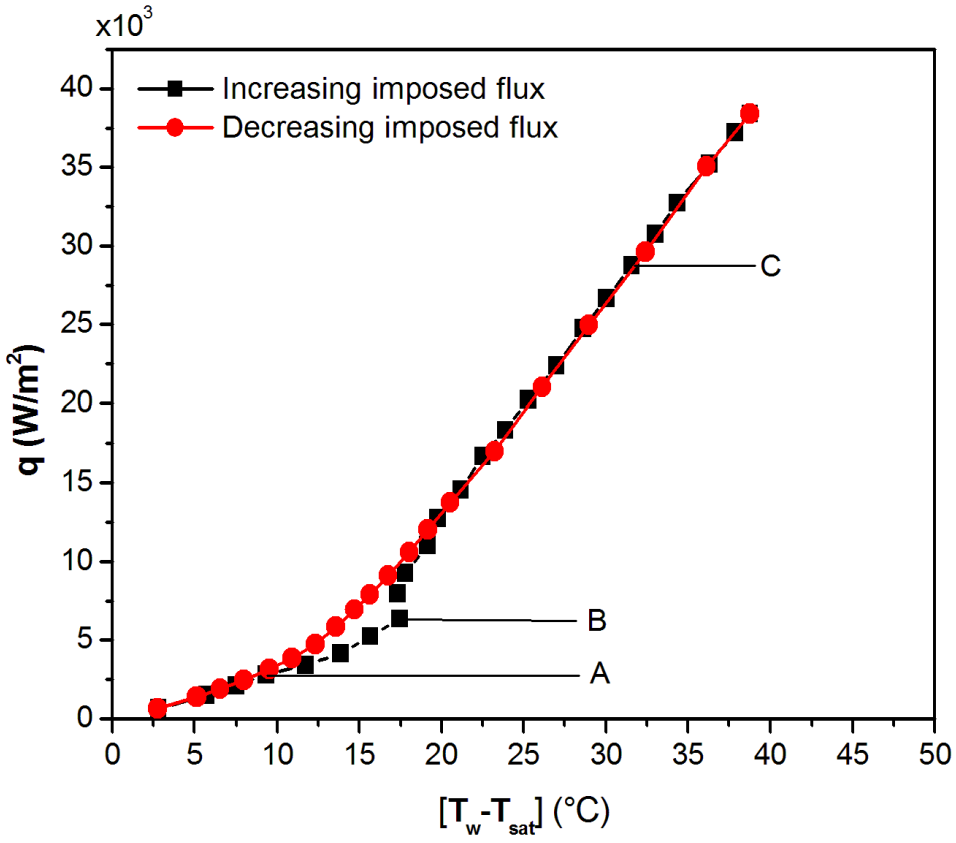

Figure 8: Heat transfer characteristic curve in case of an exploration with an ascending and a descending heat flux for FC72(T_{sat}=36°C, p_{sat}=0.48 bar). The points A, B, C correspond to the conditions retained for the presentation of the temporal evolution of the heat flux and the temperature at the wall in figure ~~8~~ 9.

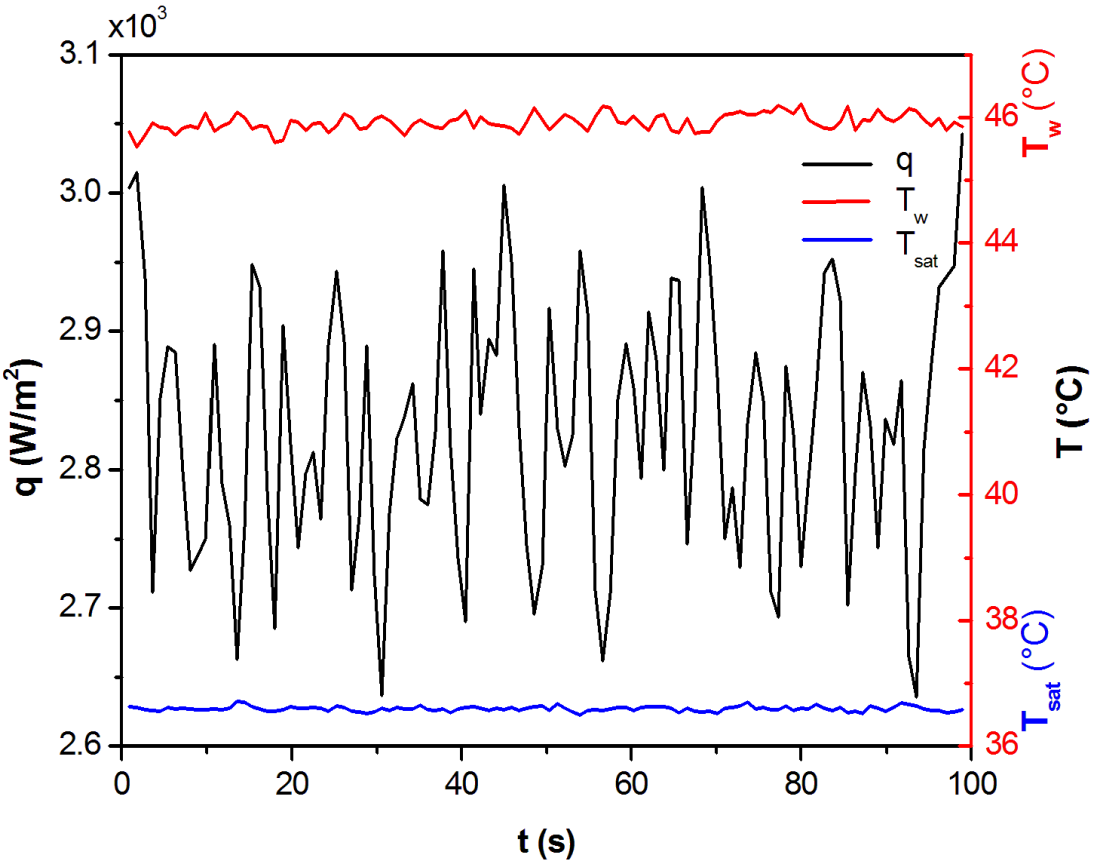

Point A in figure 8
Figure 9(a)

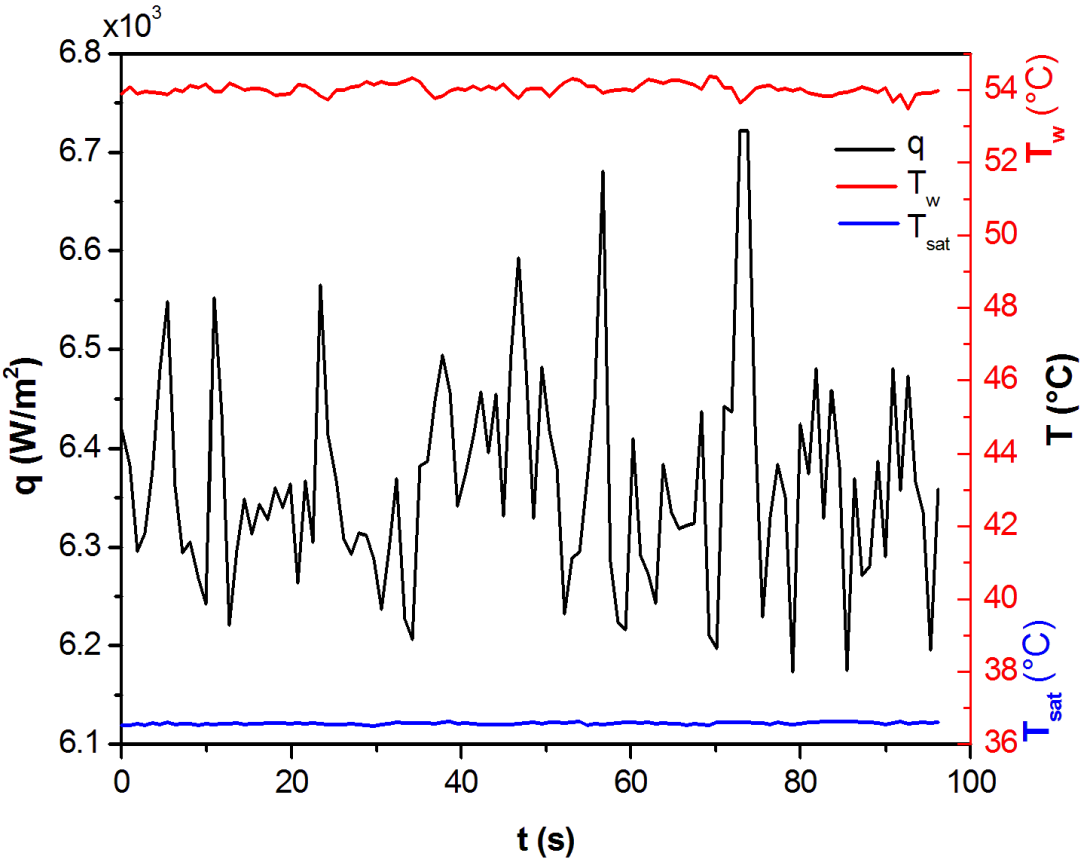

Point A in figure 8
Figure 9(b)

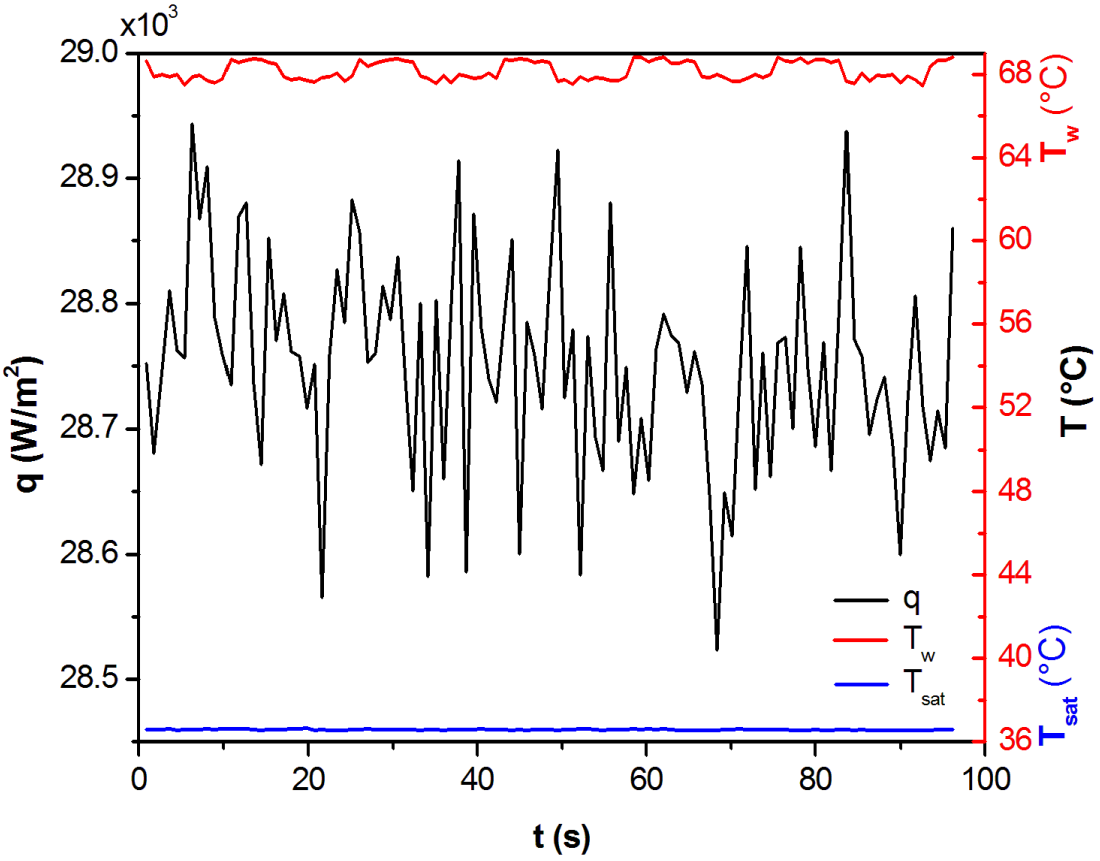

Point A in figure 8
Figure 9(c)

Figure 9: Time evolution of the heat flux and of the temperature at the boiling surface of the boiling-meter and of the pool temperature for the points A, B, C defined on the heat transfer characteristic curve in figure 8.

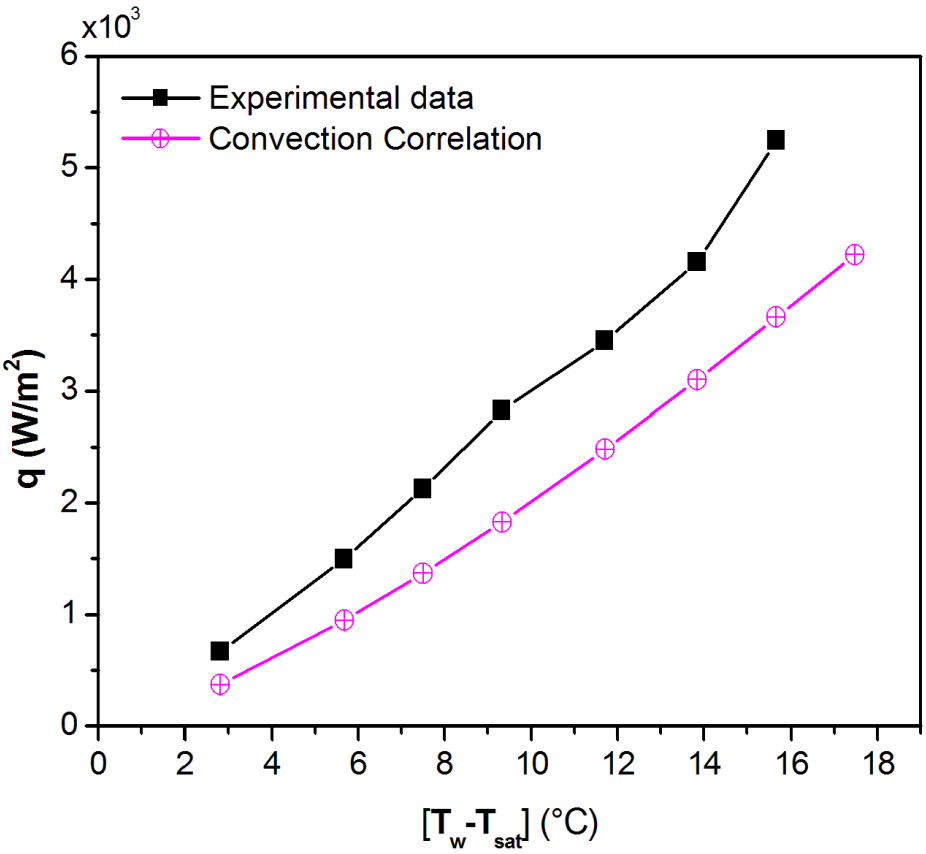

Figure 10: Heat flux variation versus the wall superheat for the saturation condition (T_{sat}=*36°C,* p_{sat}=*0.48bar)*. These experimental results are compared to those derived from the correlation for natural convection proposed by (Fujii et al.[39])

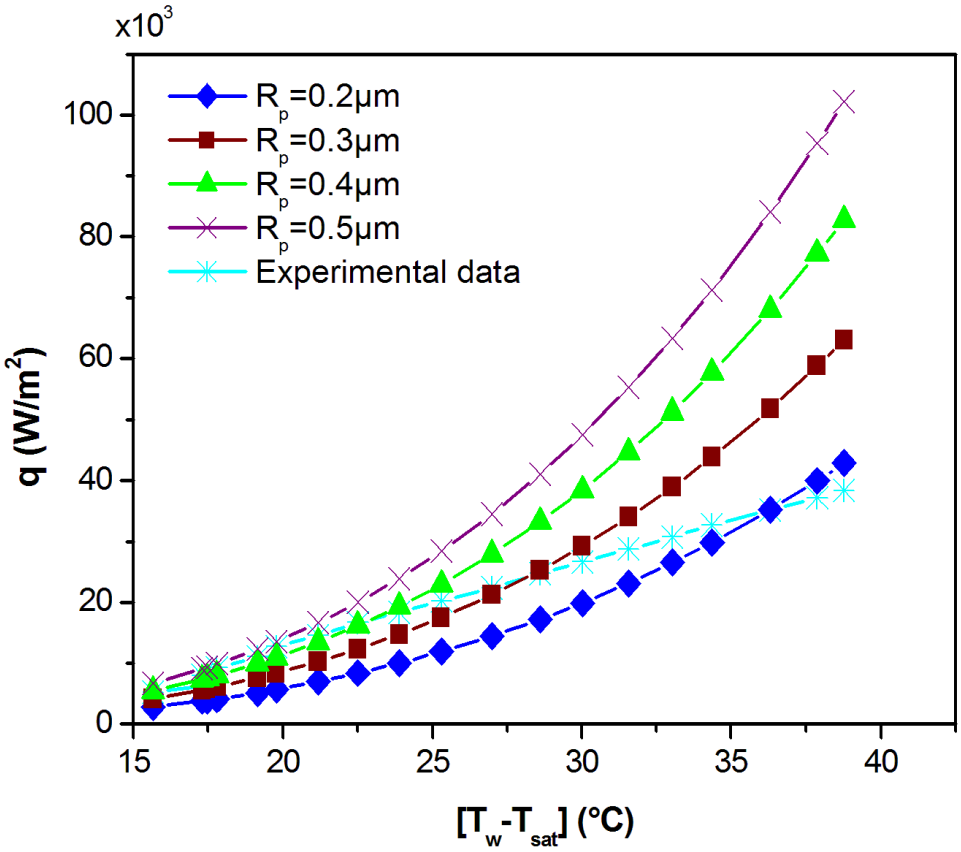

Figure 11: Boiling heat transfer curves in boiling regime determined from the Cooper's correlation with different values of the roughness parameter and experimental boiling curve for the saturation condition (T_{sat}=*36°C*, p_{sat}=*0.48bar*).

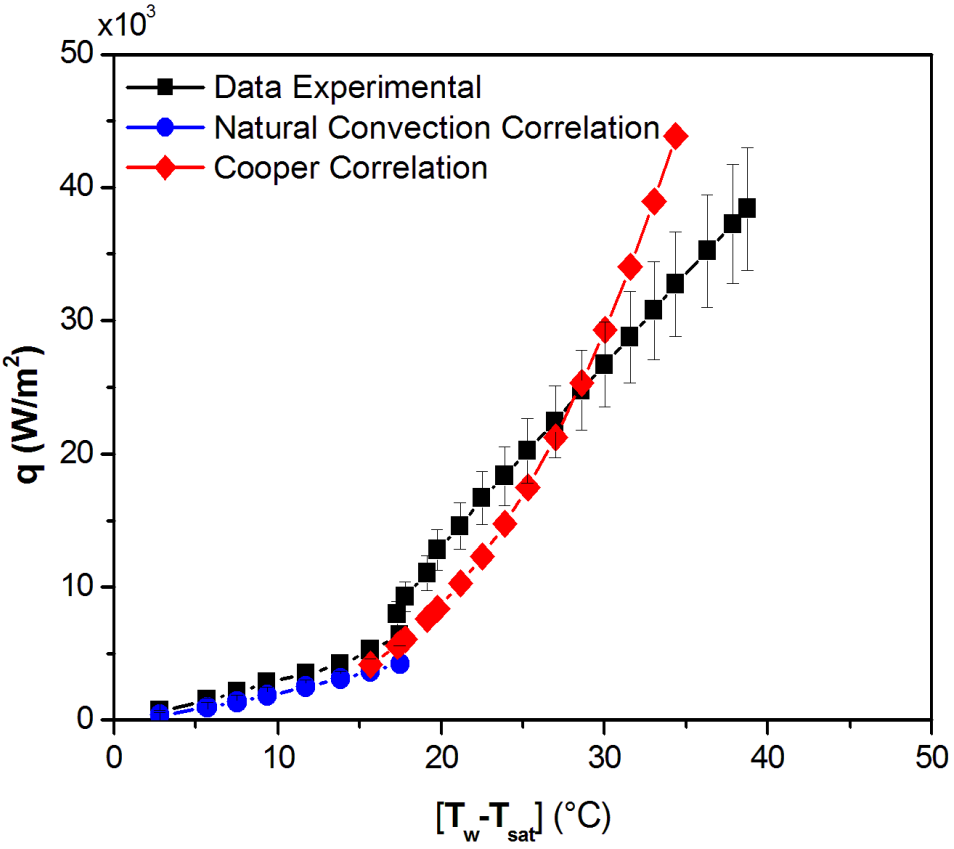

Figure 12: Heat flux versus the temperature superheat on the boiling-surface measured for the saturation condition (T_{sat}=*36°C*, P_{sat}=*0.48bar*) and calculated in the natural convection regime (blue curve) with equation (1) of Fujii et al. and in the boiling regime with the Cooper's correlation from equation (2) using a value of 0.3 µm for the roughness parameter.

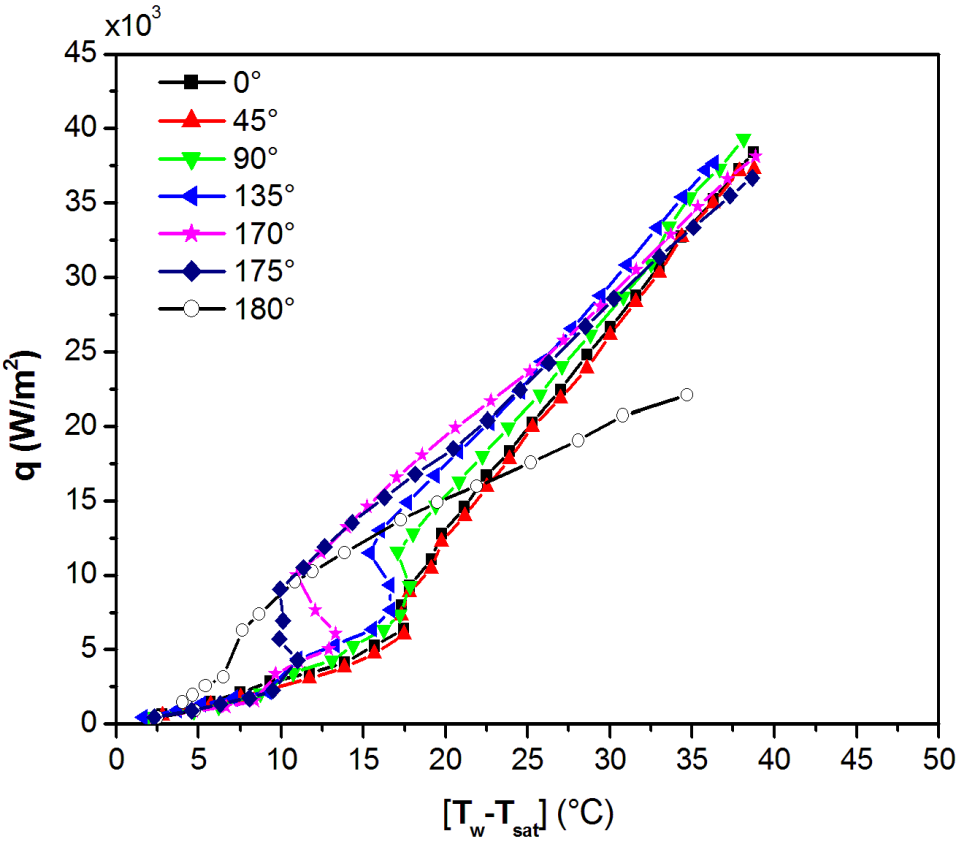

Figure 13: Characteristic heat transfer curves measured for an exploration at increasing heat flux for different tilt angles of the boiling-meter for a saturation condition: (T_{sat}=36°C, P_{sat}=0.48bar).The tilt angle is defined such as for an angle of 180°, the heated surface is horizontal and the heat flux is oriented downward and at 0°, the heated surface is horizontal and the heat flux is oriented upward.

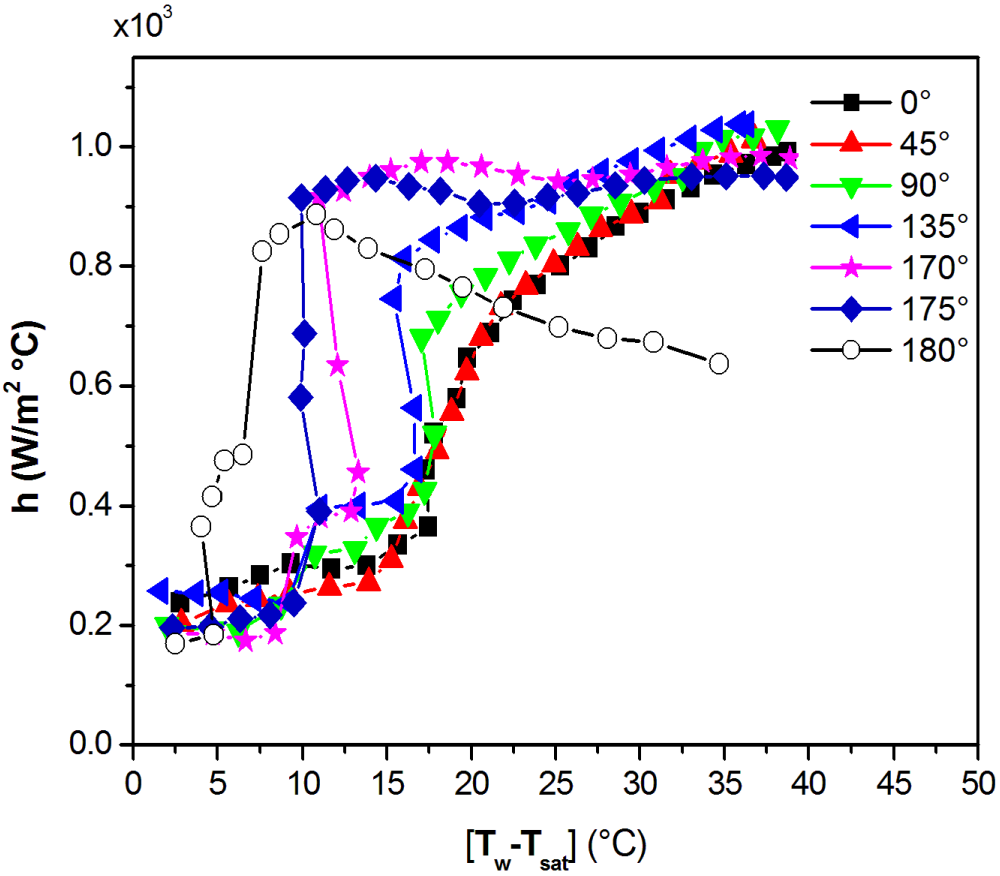

Figure 14: Heat transfer coefficient deduced from the boiling curves (fig13) measured for an exploration at increasing heat flux for different tilt angles of the boilingmeter for a saturation condition : (T_{sat}=*36°C*, p_{sat}=*0.48bar*).

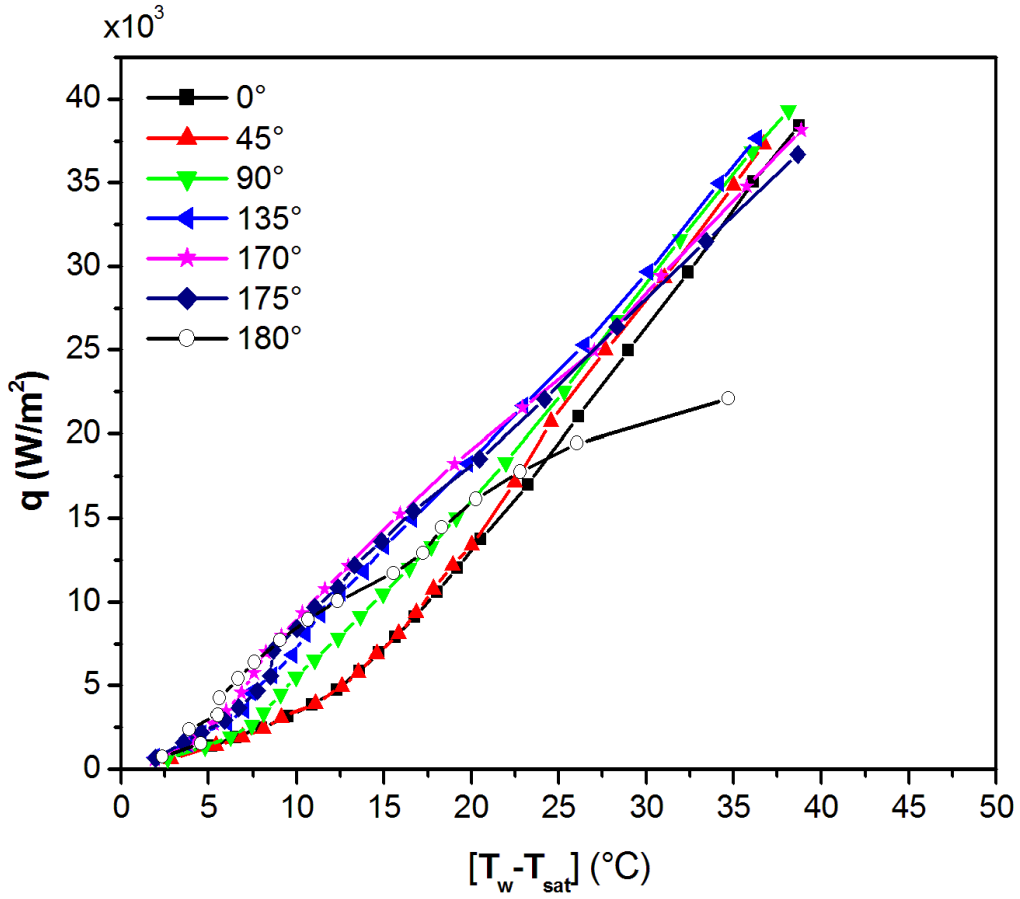

Figure 15: Characteristic heat transfer curves measured for an exploration at decreasing heat flux for different tilt angles of the boilingmeter for saturation condition (T_{sat}=36°C, p_{sat}=0.48bar).

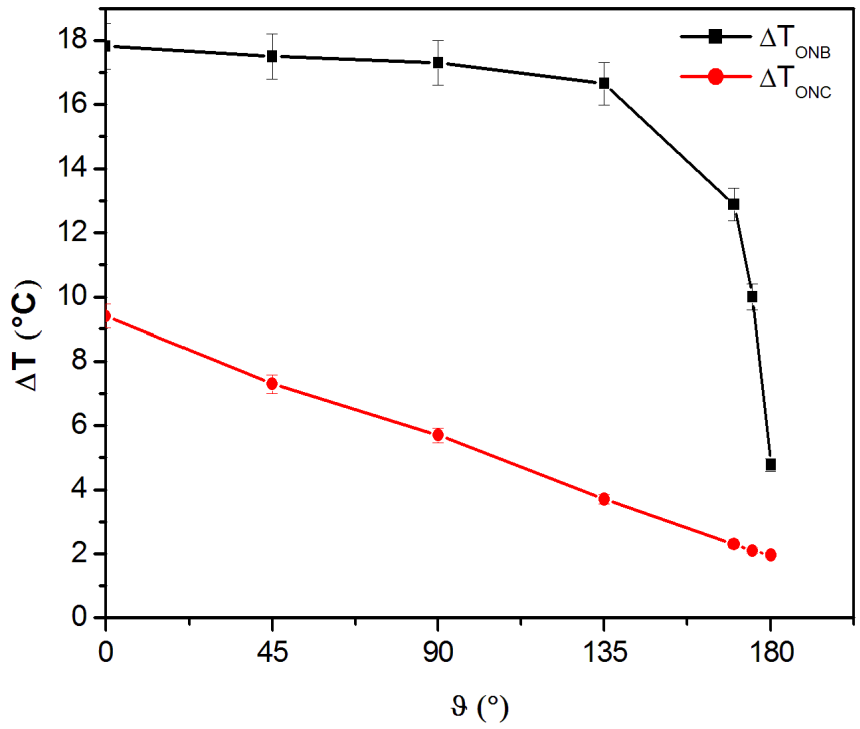

Figure 16: Onset of Nucleate Boiling ΔT_{ONB} (black curve) and Onset of Dominant Natural Convection (ONC) versus the tilt angle of the boilingmeter for a saturation condition (T_{sat}=*36°C*, P_{sat}=*0.48bar*).

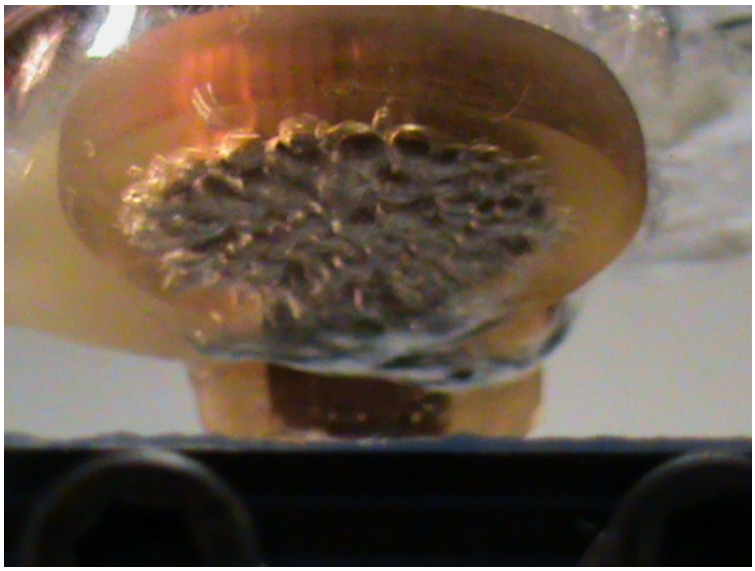

Figure 17: Photo of nucleate boiling of FC 72 at saturation condition (T_{sat}=*36°C, P_{sat}=0.48bar*) for a tilt angle of the boiling surface 180°. The heat flux q=16.000 W/m^2 and ΔT_{sat}=22 °C

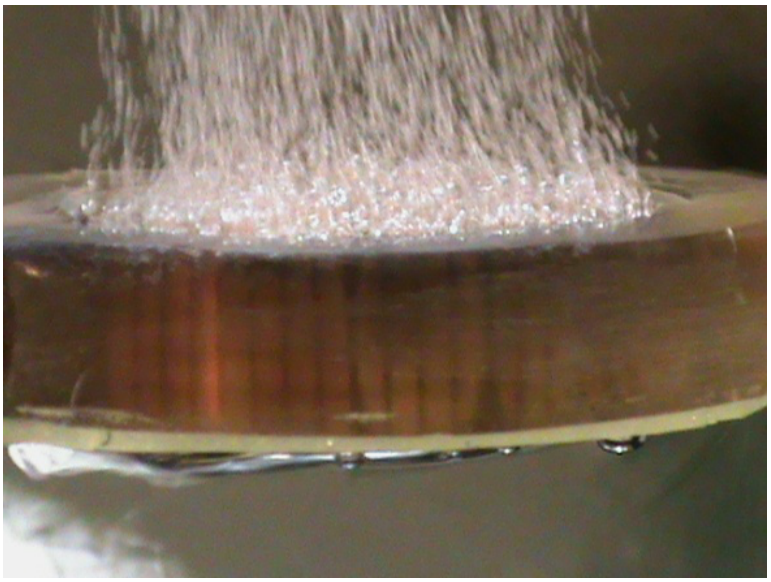

Figure 18: Photo of nucleate boiling of FC 72 at saturation condition (T_{sat}=*36°C, P_{sat}=0.48bar*) for a tilt angle of the boiling surface 0°. Heat flux q=20 253W/m^2 and ΔT_{sat}=25°C